Noname manuscript No.
(will be inserted by the editor)

Convexification of Generalized Network Flow Problem

Somayeh Sojoudi · Salar Fattahi · Javad Lavaei

Abstract This paper is concerned with the minimum-cost flow problem over an arbitrary flow network. In this problem, each node is associated with some possibly unknown injection and each line has two unknown flows at its ends that are related to each other via a nonlinear function. Moreover, all injections and flows must satisfy certain box constraints. This problem, named generalized network flow (GNF), is highly non-convex due to its nonlinear equality constraints. Under the assumption of monotonicity and convexity of the flow and cost functions, a convex relaxation is proposed, which is shown to always obtain globally optimal injections. This relaxation may fail to find optimal flows because the mapping from injections to flows is not unique in general. We show that the proposed relaxation, named convexified GNF (CGNF), obtains a globally optimal flow vector if the optimal injection vector is a Pareto point. More generally, the network can be decomposed into two subgraphs such that the lines between the subgraphs are congested at optimality and that CGNF finds correct optimal flows over all lines of one of these subgraphs. We also fully characterize the set of all globally optimal flow vectors, based on the optimal injection vector found via CGNF. In particular, we show that

Somayeh Sojoudi
Department of Industrial Engineering and Operations Research, University of California, Berkeley
E-mail: sojoudi@berkeley.edu

Salar Fattahi
Department of Industrial Engineering and Operations Research, University of California, Berkeley
E-mail: fattahi@berkeley.edu

Javad Lavaei
Department of Industrial Engineering and Operations Research, University of California, Berkeley
E-mail: lavaei@berkeley.edu

This work was supported by DARPA YFA, ONR YIP Award, AFOSR YIP Award, NSF CAREER Award 1351279 and NSF EECS Award 1406865.

this solution set is a subset of the boundary of a convex set, and may include an exponential number of disconnected components. A primary application of this work is in optimization over electrical power networks.

Keywords Network flow · Lossy networks · Convex optimization · Convex relaxation · Electrical power networks · Optimal power flow

1 Introduction

The area of "network flows" plays a central role in operations research, computer science and engineering [1,2]. This area is motivated by many real-word applications in assignment, transportation, communication networks, electrical power distribution, production scheduling, financial budgeting, and aircraft routing, to name only a few. Network flow problems have been studied extensively since 1962 [3–12]. The minimum-cost flow problem aims to optimize the flows over a flow network that is used to carry some commodity from suppliers to consumers. In a flow network, there is an injection of some commodity at every node, which leads to two flows over each line at its endpoints. The injection—depending on being positive or negative, corresponds to supply or demand at the node. The minimum-cost flow problem has been studied thoroughly for a lossless network, where the amount of flow entering a line equals the amount of flow leaving the line. However, since real-world flow networks could be lossy, the minimum-cost flow problem has also attracted much attention for generalized networks, also known as networks with gain [2,13,14]. In this type of network, each line is associated with a constant gain relating the two flows of the line through a linear function. From the optimization perspective, network flow problems are convex and can be solved efficiently, unless there are discrete variables involved [15].

There are important real-world flow networks that are lossy, where the loss is a nonlinear function of the flows. An example is electrical power networks for which the loss over each line (under fixed voltage magnitudes at both ends) is given by a parabolic function due to Kirchhoff's circuit laws [16]. The loss function could be much more complicated depending on the power electronic devices installed on the transmission line. To the best of our knowledge, there is no theoretical result in the literature on the design of efficient algorithms for network flow problems with nonlinear flow functions, except in very special cases. This paper is concerned with this general problem, named Generalized Network Flow (GNF). Note that the term "GNF" has already been used in the literature for networks with linear losses, but it corresponds to arbitrary lossy networks in this work.

GNF aims to optimize the nodal injections subject to flow constraints for each line and box constraints for both injections and flows. A flow constraint is a nonlinear equation that relates the flows at both ends of a line. To solve GNF, this paper makes the practical assumption that the cost and flow functions are all monotonic and convex. The GNF problem is still highly non-convex due to its equality constraints. However, a question arises as to whether there

is an efficient algorithm for finding globally optimal injections and flows for GNF under the assumption that the GNF problem is feasible. In this work, we prove that the answer to this question is affirmative for optimal injections (and optimal total cost), but not necessarily optimal flows. More specifically, we provide a convex relaxation of GNF that yields globally optimal injections.

Observe that relaxing the nonlinear line flow equalities to convex inequalities gives rise to a convex relaxation of GNF. It can be easily seen that solving the relaxed problem may lead to a solution for which the new inequality flow constraints are not binding. One may speculate that this observation implies that the convex relaxation is not tight. However, the objective of this work is to show that as long as GNF is feasible, the convex relaxation is tight. We also generalize the above results to the case where, other than local constraints over a line or at a node, there are global constraints relating the flows of different lines or injections of different nodes.

Although the proposed convex relaxation always finds the optimal injections (and hence the optimal objective value), it may produce wrong flows leading to non-binding inequalities. The reason behind the failure of the convex relaxation in finding globally optimal flows is that the mapping from flows to injections is not invertible. For example, it is known in the context of power systems that the power flow equations may not have a unique solution [17]. Having found the globally optimal injection vector through the proposed convex relaxation, we also study the possibility of finding optimal flows from the optimal injections. First, we prove that if the optimal injection vector is a Pareto point in its feasible region, the convex relaxation of GNF obtains globally optimal flows for GNF. Second, we show that whenever the optimal injection vector lies on the boundary of its feasible region, the flow network can be divided into two sub-networks such that: (i) the convex relaxation obtains optimal flows over one sub-network, (ii) the lines between the two sub-networks are all congested at optimality and the convex relaxation correctly identifies these lines. In other words, we relate the possible failure of the convex relaxation in finding optimal flows for the whole network to certain congested lines. Moreover, we fully characterize the set of all optimal flow vectors. In particular, we show that this set may be infinite, non-convex, and disconnected, but belongs to the boundary of a convex set.

1.1 Application of GNF in Power Systems

The operation of a power network depends heavily on various large-scale optimization problems such as state estimation, optimal power flow (OPF), security-constrained OPF, unit commitment, sizing of capacitor banks and network reconfiguration. These problems are highly non-convex due to the nonlinearities imposed by laws of physics [18, 19]. For example, each of the above problems has the power flow equations embedded in it, which are nonlinear equality constraints. The nonlinearity of OPF, as the most fundamental optimization problem for power systems, has been studied since 1962, leading

to various heuristic and local-search algorithms [20–28]. These algorithms suffer from sensitivity and convergence issues, and more importantly they may converge to a local optimum that is noticeably far from a global solution.

Recently, it has been shown in [29–31] that the semidefinite programming (SDP) relaxation is able to find a global or near-global solution of the OPF problem under a sufficient condition, which is satisfied for IEEE benchmark systems, Polish Grid with more than 3000 nodes, and many randomly generated power networks. The papers [32] and [19] prove that the satisfaction of this condition is due to the passivity of transmission lines and transformers. In particular, [19] shows that in the case where this condition is not satisfied (see [33] for counterexamples), OPF can always be solved globally in polynomial time (up to any finite precision) after two approximations: (i) relaxing angle constraints by adding a sufficient number of actual/virtual phase shifters to the network, (ii) relaxing power balance equalities to inequality constraints. OPF under Approximation (ii) was also studied in [34–36] for distribution networks. The paper [37] studies the optimization of active power flows over distribution networks under fixed voltage magnitudes and shows that the SDP relaxation works without having to use Approximation (ii) as long as a practical angle condition is satisfied.

The idea of convex relaxation developed in [38] and [29] can be applied to many other power problems, such as voltage regulation [39], energy storage [40], state estimation [41, 42], sensor placement [43], calculation of voltage stability margin [44], charging of electric vehicles [45], security constrained OPF with possibly variable tap-changers and capacitor banks [31,46], dynamic energy management [16] and electricity market [47]. In the same vein, [48] and [49] combine a convex relaxation of the power flow equations with iterative approaches to reduce the complexity of the semidefinite programming and to address certain problems in power systems that include discrete variables, such as unit commitment and optimal transmission switching problems [50, 51]. Although the SDP relaxation has been shown to be exact in several real-world examples, [33] demonstrates that this relaxation may fail in some instances. To improve upon the SDP relaxation for such cases, [52] and [53] use a hierarchy of semidefinite relaxations, known as *Lasserre* hierarchy [54], which obtain global minima of the OPF problem at the expense of a higher computational complexity. The paper [55] proves that in the case where the SDP relaxation is not exact, it still has a low-rank solution whose rank is upper bounded by the treewidth of the power system plus one.

Energy-related optimization problems with embedded power flow equations can be regarded as nonlinear network flow problems, which are analogous to GNF. The results derived in this work for a general GNF problem lead to the generalization of the result of [36] to networks with virtual phase shifters. This proves that in order to use SDP relaxations for OPF over an arbitrary power network, it is not needed to approximate power balance equalities with inequality constraints (under a practical angle assumption).

1.2 Notations

The following notations will be used throughout this paper:

- $\mathbb{R}$ and $\mathbb{R}_+$ denote the sets of real numbers and nonnegative numbers, respectively.
- Given two matrices M and N, the inequality $M \leq N$ means that M is less than or equal to N element-wise.
- Given a set $\mathcal{T}$, its cardinality is shown as $|\mathcal{T}|$.
- Lowercase, bold lowercase and uppercase letters are used for scalars, vectors and matrices (e.g., x, $\mathbf{x}$ and X). The i^{th} entry of a vector $\mathbf{x}$ is shown as x_i. Likewise, the $(i,j)^{\text{th}}$ entry of a matrix X is denoted as X_{ij}.
- Given a nonconvex optimization problem, the term "**solution**" is short for "**globally optimal solution**" henceforth (because local minima are not of interest in this work).

2 Problem Statement and Contributions

Consider an undirected graph (network) $\mathcal{G}$ with the vertex set $\mathcal{N} := \{1, 2, ..., m\}$ and the edge set $\mathcal{E} \subseteq \mathcal{N} \times \mathcal{N}$. For every $i \in \mathcal{N}$, let $\mathcal{N}(i)$ denote the set of the neighboring vertices of node i. Assume that every edge $(i,j) \in \mathcal{E}$ is associated with two unknown flows p_{ij} and p_{ji} belonging to $\mathbb{R}$. The parameters p_{ij} and p_{ji} can be regarded as the flows entering the edge (i,j) from the endpoints i and j, respectively. Define

$$p_i = \sum_{j \in \mathcal{N}(i)} p_{ij}, \qquad \forall i \in \mathcal{N} \tag{1}$$

The parameter p_i is called "nodal injection at vertex i" or simply "injection", which is equal to the sum of the flows leaving vertex i through the edges connected to this vertex. Given an edge $(i,j) \in \mathcal{E}$, we assume that the flows p_{ij} and p_{ji} are related to each other via a function $f_{ij}(\cdot)$ to be introduced later. To specify which of the flows p_{ij} and p_{ji} is a function of the other, we give an arbitrary orientation to every edge of the graph $\mathcal{G}$ and denote the resulting graph as $\overrightarrow{\mathcal{G}}$. Denote the directed edge (arc) set of $\overrightarrow{\mathcal{G}}$ as $\overrightarrow{\mathcal{E}}$. If an edge $(i,j) \in \mathcal{E}$ belongs to $\overrightarrow{\mathcal{E}}$, we then express p_{ji} as a function of p_{ij}.

Definition 1 *Define the vectors* $\mathbf{p}_n$, $\mathbf{p}_e$ *and* $\mathbf{p}_d$ *as follows:*

$$\mathbf{p}_n = \{p_i \mid \forall i \in \mathcal{N}\} \tag{2a}$$

$$\mathbf{p}_e = \{p_{ij} \mid \forall (i,j) \in \mathcal{E}\} \tag{2b}$$

$$\mathbf{p}_d = \{p_{ij} \mid \forall (i,j) \in \overrightarrow{\mathcal{E}}\} \tag{2c}$$

(the subscripts "n", "e" and "d" stand for nodes, edges and directed edges). The terms $\mathbf{p}_n$, $\mathbf{p}_e$ *and* $\mathbf{p}_d$ *are referred to as* injection vector, flow vector *and* semi-flow vector, *respectively (note that* $\mathbf{p}_e$ *contains two flows per each line, whereas* $\mathbf{p}_d$ *includes only one flow per line).*

Definition 2 *Given two arbitrary points* $\mathbf{x}, \mathbf{y} \in \mathbb{R}^n$*, the box* $\mathcal{B}(\mathbf{x}, \mathbf{y})$ *is defined as follows:*

$$B(\mathbf{x}, \mathbf{y}) = \{\mathbf{z} \in \mathbb{R}^n \ | \mathbf{x} \leq \mathbf{z} \leq \mathbf{y}\} \tag{3}$$

(note that $B(\mathbf{x}, \mathbf{y})$ *is non-empty only if* $\mathbf{x} \leq \mathbf{y}$*).*

Assume that each injection p_i and each flow p_{ij} must be within the pre-specified intervals $[p_i^{\min}, p_i^{\max}]$ and $[p_{ij}^{\min}, p_{ij}^{\max}]$, respectively, for every $i \in \mathcal{N}$ and $(i,j) \in \overrightarrow{\mathcal{E}}$. We use the shorthand notation $\mathcal{B}$ for the box $\mathcal{B}(\mathbf{p}_n^{\min}, \mathbf{p}_n^{\max})$, where $\mathbf{p}_n^{\min}$ and $\mathbf{p}_n^{\max}$ are the vectors of the lower bounds $p_i^{\min}$'s and the upper bounds $p_i^{\max}$'s, respectively.

This paper is concerned with the following problem.

Generalized network flow (GNF) Problem:

$$\min_{\mathbf{p}_n \in \mathcal{B}, \mathbf{p}_e \in \mathbb{R}^{|\mathcal{E}|}} \quad \sum_{i \in \mathcal{N}} f_i(p_i) \tag{4a}$$

$$\text{subject to} \quad p_i = \sum_{j \in \mathcal{N}(i)} p_{ij}, \qquad \forall i \in \mathcal{N} \tag{4b}$$

$$p_{ji} = f_{ij}(p_{ij}), \qquad \forall (i,j) \in \overrightarrow{\mathcal{E}} \tag{4c}$$

$$p_{ij} \in [p_{ij}^{\min}, p_{ij}^{\max}], \qquad \forall (i,j) \in \overrightarrow{\mathcal{E}} \tag{4d}$$

where

1) $f_i(\cdot)$ *is convex and strictly increasing for every* $i \in \mathcal{N}$*.*
2) $f_{ij}(\cdot)$ *is convex and strictly decreasing for every* $(i,j) \in \overrightarrow{\mathcal{E}}$*.*
3) The limits $p_{ij}^{\min}$ *and* $p_{ij}^{\max}$ *are given for every* $(i,j) \in \overrightarrow{\mathcal{E}}$*.*

In the case where $f_{ij}(p_{ij})$ is equal to $-p_{ij}$ for all $(i,j) \in \overrightarrow{\mathcal{E}}$, the GNF problem reduces to the network flow problem for which every line is lossless. A few remarks can be made here:

- Given an edge $(i,j) \in \overrightarrow{\mathcal{E}}$, there is no explicit limit on p_{ji} in the above formulation of the GNF problem because any such constraint can be equivalently imposed on p_{ij}.
- Given a node $i \in \mathcal{N}$, the assumption of $f_i(p_i)$ being monotonically increasing is motivated by the fact that increasing the injection p_i normally elevates the cost in practice.
- Given an edge $(i,j) \in \overrightarrow{\mathcal{E}}$, p_{ij} and $-p_{ji}$ can be regarded as the input and output flows of the line (i,j) traveling in the same direction. The assumption of $f_{ij}(p_{ij})$ being monotonically decreasing is motivated by the fact that increasing the input flow normally makes the output flow higher in practice (note that $-p_{ji} = -f_{ij}(p_{ij})$).

Definition 3 *Define* $\mathcal{P}$ *as the set of all vectors* $\mathbf{p}_n$ *for which there exists a vector* $\mathbf{p}_e$ *such that* $(\mathbf{p}_n, \mathbf{p}_e)$ *satisfies equations (4b), (4c) and (4d). The set* $\mathcal{P}$ *and* $\mathcal{P} \cap \mathcal{B}$ *are referred to as* injection region *and* box-constrained injection region*, respectively.*

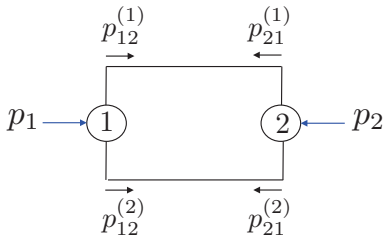

Fig. 1: The graph $\mathcal{G}$ studied in Section 3.1.

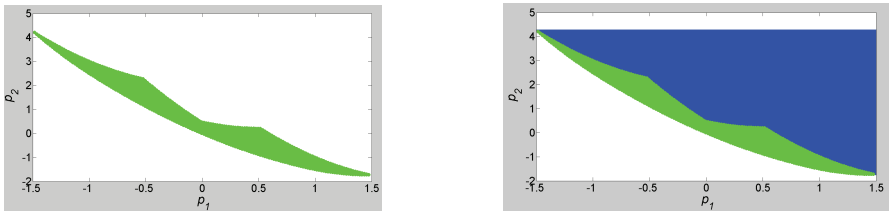

(a) (b)

Fig. 2: (a) Injection region $\mathcal{P}$ for the GNF problem given in (8); (b): the set $\mathcal{P}_c$ corresponding to the GNF problem given in (8).

Regarding Definition 3, the box-constrained injection region is indeed the projection of the feasible set of GNF onto the space for the injection vector $\mathbf{p}_n$. We express GNF geometrically as follows:

$$\text{Geometric GNF}: \quad \min_{\mathbf{p}_n \in \mathcal{P} \cap \mathcal{B}} \sum_{i \in \mathcal{N}} f_i(p_i) \tag{5}$$

Note that $\mathbf{p}_e$ has been eliminated in Geometric GNF. It is hard to solve this problem directly because the injection region $\mathcal{P}$ is non-convex in general. This non-convexity can be observed in Figure 2(a), which shows $\mathcal{P}$ for the two-node graph drawn in Figure 1. To address this non-convexity issue, the GNF problem will be convexified next.

Convexified generalized network flow (CGNF) Problem:

$$\min_{\mathbf{P}_n \in \mathcal{B}, \mathbf{P}_e \in \mathbb{R}^{|\mathcal{E}|}} \quad \sum_{i \in \mathcal{N}} f_i(p_i) \tag{6a}$$

$$\textit{subject to} \quad p_i = \sum_{j \in \mathcal{N}(i)} p_{ij}, \qquad \forall i \in \mathcal{N} \tag{6b}$$

$$p_{ji} \geq f_{ij}(p_{ij}), \qquad \forall (i,j) \in \overrightarrow{\mathcal{E}} \tag{6c}$$

$$p_{ij} \in [p_{ij}^{\min}, p_{ij}^{\max}], \qquad \forall (i,j) \in \mathcal{E} \tag{6d}$$

where $(p_{ij}^{\min}, p_{ij}^{\max})$ *is defined as* $(f_{ji}(p_{ji}^{\max}), f_{ji}(p_{ji}^{\min}))$ *for every* $(i,j) \in \mathcal{E}$ *such that* $(j,i) \in \overrightarrow{\mathcal{E}}$.

CGNF has been obtained from GNF by relaxing equality (4c) to inequality (6c) and adding limits to p_{ij} for every $(j,i) \in \overrightarrow{\mathcal{E}}$. One can write:

$$\text{Geometric CGNF}: \quad \min_{\mathbf{p}_n \in \mathcal{P}_c \cap \mathcal{B}} \sum_{i \in \mathcal{N}} f_i(p_i) \tag{7}$$

where $\mathcal{P}_c$ denotes the set of all vectors $\mathbf{p}_n$ for which there exists a vector $\mathbf{p}_e$ such that $(\mathbf{p}_n, \mathbf{p}_e)$ satisfies equations (6b), (6c) and (6d). Two main results to be proved in this paper are:

- **Geometry of injection region:** Given any two points $\mathbf{p}_n$ and $\tilde{\mathbf{p}}_n$ in the injection region, the box $\mathcal{B}(\mathbf{p}_n, \tilde{\mathbf{p}}_n)$ is entirely contained in the injection region. A similar result holds true for the box-constrained injection region.
- **Relationship between GNF and CGNF:** Using the above result on the geometry of the injection region, we show that if $(\mathbf{p}_n^*, \mathbf{p}_e^*)$ and $(\bar{\mathbf{p}}_n^*, \bar{\mathbf{p}}_e^*)$ denote two arbitrary solutions of GNF and CGNF, then $\mathbf{p}_n^* = \bar{\mathbf{p}}_n^*$. Hence, CGNF always finds the correct optimal injection vector for GNF. Moreover, $(\bar{\mathbf{p}}_n^*, \bar{\mathbf{p}}_e^*)$ is a solution of GNF as well if $\mathbf{p}_n^*$ is a Pareto point in $\mathcal{P}$. More generally, if $\mathbf{p}_n^*$ resides on the boundary of $\mathcal{P}$, but is not necessarily a Pareto point, CGNF finds the correct optimal flows for a non-empty subgraph of $\mathcal{G}$.

Furthermore, the above results are generalized to an extended GNF problem, where there are global constraints coupling the flows or injections of different parts of the network. In particular, it is proved that the technique developed for the GNF problem works for the extended GNF problem as well, provided that the coupling constraints are convex and preserve a box-preserving property. Note that this work implicitly assumes that every two nodes of $\mathcal{G}$ are connected via at most one edge. However, the results to be derived later are all valid in the presence of multiple edges between two nodes. To avoid complicated notations, the proof will not be provided for this case. However, Section 3.1 will analyze a simple example with parallel lines.

3 Main Results

In this section, we first provide a detailed illustrative example to clarify the non-convexity issue and highlight some of the contributions of this paper. The main results for GNF and CGNF problems are developed in Subsections 3.2 and 3.3, respectively. The set of all optimal flow vectors is charaterized in Subsection 3.4. The generalization to the extended GNF problem is provided in Subsection 3.5. Finally, the application of the developed methodology in power systems is discussed in Subsection 3.6.

3.1 Illustrative Example

In this subsection, we study the particular graph $\mathcal{G}$ depicted in Figure 1. This graph has two vertices and two parallel edges. Let $(p_{12}^{(1)}, p_{21}^{(1)})$ and $(p_{12}^{(2)}, p_{21}^{(2)})$

denote the flows associated with the first and second edges of the graph, respectively. Consider the GNF problem

$$\begin{aligned} \min \quad & f_1(p_1) + f_2(p_2) && \text{(8a)} \\ \text{s.t.} \quad & p_{21}^{(i)} = \left(p_{12}^{(i)} - 1\right)^2 - 1, \qquad \forall i \in \{1,2\} && \text{(8b)} \\ & -0.5 \le p_{12}^{(1)} \le 0.5, \quad -1 \le p_{12}^{(2)} \le 1, && \text{(8c)} \\ & p_1 = p_{12}^{(1)} + p_{12}^{(2)}, \quad p_2 = p_{21}^{(1)} + p_{21}^{(2)} && \text{(8d)} \end{aligned}$$

with the variables $p_1, p_2, p_{12}^{(1)}, p_{21}^{(1)}, p_{12}^{(2)}, p_{21}^{(2)}$, where $f_1(\cdot)$ and $f_2(\cdot)$ are arbitrary convex and monotonically increasing functions. The CGNF problem corresponding to this problem can be obtained by replacing (8b) with $p_{21}^{(i)} \ge (p_{12}^{(i)} - 1)^2 - 1$ and adding the limits $p_{21}^{(1)} \le 1.5^2 - 1$ and $p_{21}^{(2)} \le 2^2 - 1$. One can write:

$$\text{Geometric GNF:} \quad \min_{(p_1,p_2)\in\mathcal{P}} f_1(p_1) + f_2(p_2) \tag{9a}$$

$$\text{Geometric CGNF:} \quad \min_{(p_1,p_2)\in\mathcal{P}_c} f_1(p_1) + f_2(p_2) \tag{9b}$$

where $\mathcal{P}$ and $\mathcal{P}_c$ are indeed the projections of the feasible sets of GNF and CGNF over the injection space for (p_1, p_2) (note that there is no box constraint on (p_1, p_2) at this point). The green area in Figure 2(a) shows the injection region $\mathcal{P}$. As expected, this set is non-convex. In contrast, the set $\mathcal{P}_c$ is a convex set containing $\mathcal{P}$. This set is shown in Figure 2(b), which includes two parts: (i) the green area that is the same as $\mathcal{P}$, (ii) the blue area that is the part of $\mathcal{P}_c$ that does not exist in $\mathcal{P}$. Thus, the transition from GNF to CGNF extends the injection region $\mathcal{P}$ to a convex set by adding the blue area. Notice that $\mathcal{P}_c$ has three boundaries: (i) a straight line on the top, (ii) a straight line on the right side, (iii) a lower curvy boundary. Since $f_1(\cdot)$ and $f_2(\cdot)$ are both monotonically increasing, the unique solution of Geometric CGNF must lie on the lower curvy boundary of $\mathcal{P}_c$. Since this lower boundary is in the green area, it is contained in $\mathcal{P}$. As a result, the unique solution of Geometric CGNF is a feasible point of $\mathcal{P}$ and therefore it is a solution of Geometric GNF. This means that CGNF finds the optimal injection vector for GNF.

To make the problem more interesting, we add the box constraint $(p_1, p_2) \in \mathcal{B}$ to GNF (and correspondingly to CGNF), where $\mathcal{B}$ is an arbitrary rectangular convex set in $\mathbb{R}^2$. The effect of this box constraint will be investigated in four different scenarios:

- Assume that $\mathcal{B}$ corresponds to Box 1 (including its interior) in Figure 3(a). In this case, $\mathcal{P} \cap \mathcal{B} = \mathcal{P}_c \cap \mathcal{B} = \phi$, implying that Geometric GNF and Geometric CGNF are both infeasible.
- Assume that $\mathcal{B}$ corresponds to Box 2 (including its interior) in Figure 3(a). In this case, the solution of Geometric CGNF lies on the lower boundary of $\mathcal{P}_c$ and therefore it is also a solution of Geometric GNF.

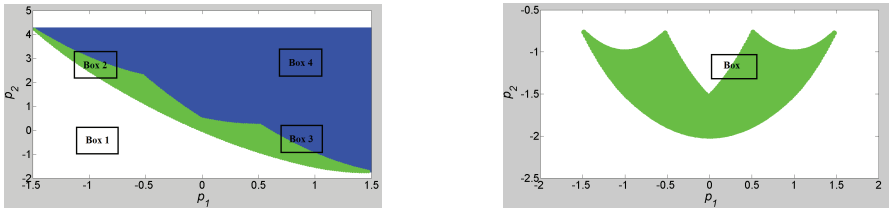

(a) (b)

Fig. 3: (a): This figure shows the set $\mathcal{P}_c$ corresponding to the GNF problem given in (8) together with a box constraint $(p_1, p_2) \in \mathcal{B}$ for four different positions of $\mathcal{B}$; (b) this figure shows the injection region $\mathcal{P}$ for the GNF problem given in (8) but after changing (8b) to (10).

- Assume that $\mathcal{B}$ corresponds to Box 3 (including its interior) in Figure 3(a). In this case, the solutions of Geometric GNF and Geometric CGNF are identical and both correspond to the lower left corner of the box $\mathcal{B}$.
- Assume that $\mathcal{B}$ corresponds to Box 4 (including its interior) in Figure 3(a). In this case, $\mathcal{P} \cap \mathcal{B} = \phi$ but $\mathcal{P}_c \cap \mathcal{B} \neq \phi$. Hence, Geometric GNF is infeasible while Geometric CGNF has an optimal solution.

In summary, it can be argued that, independent of the position of the box $\mathcal{B}$ in $\mathbb{R}^2$, CGNF finds the optimal injection vector for GNF as long as GNF is feasible.

Now, suppose that the relationship between $p_{21}^{(i)}$ and $p_{12}^{(i)}$ is governed by

$$p_{21}^{(i)} = \left(p_{12}^{(i)}\right)^2 - 1, \qquad \forall i \in \{1, 2\} \tag{10}$$

instead of (8b). The injection region $\mathcal{P}$ in the case is depicted in Figure 3(b). As before, we impose a box constraint $(p_1, p_2) \in \mathcal{B}$ on GNF, where $\mathcal{B}$ is shown as "Box" in the figure. It is easy to show that the lower left corner of this box belongs to $\mathcal{P}_c$ and hence it is a solution of Geometric CGNF. However, this corner point does not belong to Geometric GNF. More precisely, Geometric GNF is feasible in this case, while its solution does not coincide with that of Geometric CGNF. Hence, Geometric GNF and Geometric CGNF are no longer equivalent after changing (8b) to (10). This is a consequence of the fact that the function $(p-1)^2 - 1$ is decreasing in p over the interval $[-1, 1]$ while the function $p^2 - 1$ is not. This explains the necessity of the assumption of the monotonicity of $f_{ij}(\cdot)$ made earlier in the paper.

3.2 Geometry of Injection Region

In order to study the relationship between GNF and CGNF, it is beneficial to explore the geometry of the feasible set of GNF. Hence, we investigate the

geometry of the injection region $\mathcal{P}$ and the box-constrained injection region $\mathcal{P} \cap \mathcal{B}$ in this part.

Theorem 1 *Consider two arbitrary points $\hat{\mathbf{p}}_n$ and $\tilde{\mathbf{p}}_n$ in the injection region $\mathcal{P}$. The box $\mathcal{B}(\hat{\mathbf{p}}_n, \tilde{\mathbf{p}}_n)$ is contained in $\mathcal{P}$.* ■

The proof of this theorem is based on four lemmas, and will be provided later in this subsection. To understand this theorem, consider the injection region $\mathcal{P}$ depicted in Figure 2(a) corresponding to the illustrative example given in Section 3.1. If any arbitrary box is drawn in $\mathbb{R}^2$ in such a way that its upper right corner and lower left corner both lie in the green area, then the entire box must lie in the green area completely. This can be easily proved in this special case and is true in general due to Theorem 1. However, this result does not hold for the injection region given in Figure 3(b) because the assumption of monotonicity of $f_{ij}(\cdot)$'s is violated in this case. The result of Theorem 1 can be generalized to the box-constrained injection region, as stated below.

Corollary 1 *Consider two arbitrary points $\hat{\mathbf{p}}_n$ and $\tilde{\mathbf{p}}_n$ belonging to the box-constrained injection region $\mathcal{P} \cap \mathcal{B}$. The box $\mathcal{B}(\hat{\mathbf{p}}_n, \tilde{\mathbf{p}}_n)$ is contained in $\mathcal{P} \cap \mathcal{B}$.*

Proof: The proof follows immediately from Theorem 1. ■

The rest of this subsection is dedicated to the proof of Theorem 1, which is based on a series of definitions and lemmas.

Definition 4 *Define $\mathcal{B}_d$ as the box containing all vectors $\mathbf{p}_d$ introduced in (2c) that satisfy the condition $p_{ij} \in [p_{ij}^{\min}, p_{ij}^{\max}]$ for every $(i,j) \in \overrightarrow{\mathcal{E}}$.*

Definition 5 *It is said that $\mathbf{p}_d$ is associated with $\mathbf{p}_n$, or vice versa, if $(\mathbf{p}_n, \mathbf{p}_d)$ is feasible for the GNF problem. Likewise, $\mathbf{p}_e$ is associated with $\mathbf{p}_n$ if $(\mathbf{p}_n, \mathbf{p}_e)$ is feasible for the CGNF problem.*

Definition 6 *Given two arbitrary points $\bar{\mathbf{p}}_d, \tilde{\mathbf{p}}_d \in \mathcal{B}_d$, define $M(\bar{\mathbf{p}}_d, \tilde{\mathbf{p}}_d)$ according to the following procedure:*

- *Let $M(\bar{\mathbf{p}}_d, \tilde{\mathbf{p}}_d)$ be a matrix with $|\mathcal{N}|$ rows indexed by the vertices of $\mathcal{G}$ and with $|\overrightarrow{\mathcal{E}}|$ columns indexed by the edges in $\overrightarrow{\mathcal{E}}$.*
- *For every vertex $k \in \mathcal{N}$ and edge $(i,j) \in \overrightarrow{\mathcal{E}}$, set the $(k,(i,j))^{th}$ entry of $M(\bar{\mathbf{p}}_d, \tilde{\mathbf{p}}_d)$ (the one in the intersection of row k and column (i,j)) as*

$$\begin{cases} 1 & \text{if} \quad k = i \\ \frac{f_{ij}(\bar{p}_{ij}) - f_{ij}(\tilde{p}_{ij})}{\bar{p}_{ij} - \tilde{p}_{ij}} & \text{if} \quad k = j \text{ and } \bar{p}_{ij} \neq \tilde{p}_{ij} \\ f'_{ij}(\bar{p}_{ij}) & \text{if} \quad k = j \text{ and } \bar{p}_{ij} = \tilde{p}_{ij} \\ 0 & \text{otherwise} \end{cases} \tag{11}$$

where $f'_{ij}(\bar{p}_{ij})$ denotes the right derivative of $f_{ij}(\bar{p}_{ij})$ if $\bar{p}_{ij} < p_{ij}^{max}$ and the left derivative of $f_{ij}(\bar{p}_{ij})$ if $\bar{p}_{ij} = p_{ij}^{max}$.

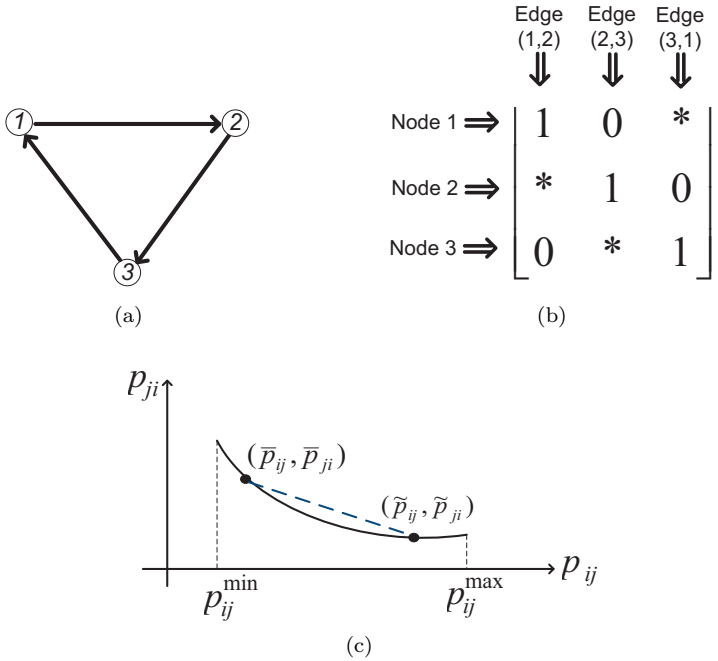

Fig. 4: (a) A particular graph $\mathcal{G}$; (b) the matrix $M(\bar{\mathbf{p}}_d, \tilde{\mathbf{p}}_d)$ corresponding to the graph $\mathcal{G}$ in Figure 4(a); (c): the $(j,(i,j))^{\text{th}}$ entry of $M(\bar{\mathbf{p}}_d, \tilde{\mathbf{p}}_d)$ (shown as "*") is equal to the slope of the line connecting the points $(\bar{p}_{ij}, \bar{p}_{ji})$ and $(\tilde{p}_{ij}, \tilde{p}_{ji})$.

To illustrate Definition 6, consider the three-node graph $\overrightarrow{\mathcal{G}}$ depicted in Figure 4(a). The matrix $M(\bar{\mathbf{p}}_d, \tilde{\mathbf{p}}_d)$ associated with this graph has the structure shown in Figure 4(b), where the "*" entries depend on the specific values of $\bar{\mathbf{p}}_d$ and $\tilde{\mathbf{p}}_d$. Consider an edge $(i,j) \in \overrightarrow{\mathcal{E}}$. The $(j,(i,j))^{\text{th}}$ entry of $M(\bar{\mathbf{p}}_d, \tilde{\mathbf{p}}_d)$ is equal to

$$\frac{f_{ij}(\bar{p}_{ij}) - f_{ij}(\tilde{p}_{ij})}{\bar{p}_{ij} - \tilde{p}_{ij}}, \tag{12}$$

provided $\bar{p}_{ij} \neq \tilde{p}_{ij}$. As can be seen in Figure 4(c), this is equal to the slope of the line connecting the point $(\bar{p}_{ij}, \bar{p}_{ji})$ to the point $(\tilde{p}_{ij}, \tilde{p}_{ji})$ on the parameterized curve (p_{ij}, p_{ji}), where $p_{ji} = f_{ij}(p_{ij})$. Moreover, $f'_{ij}(\bar{p}_{ij})$ is the limit of this slope as the point $(\tilde{p}_{ij}, \tilde{p}_{ji})$ approaches $(\bar{p}_{ij}, \bar{p}_{ji})$. It is also interesting to note that $M(\bar{\mathbf{p}}_d, \tilde{\mathbf{p}}_d)$ has one positive entry, one negative entry and $m-2$ zero entries in each column (note that the slope of the line connecting $(\bar{p}_{ij}, \bar{p}_{ji})$ to $(\tilde{p}_{ij}, \tilde{p}_{ji})$ is always negative). The next lemma explains how the matrix $M(\bar{\mathbf{p}}_d, \tilde{\mathbf{p}}_d)$ can be used to relate the semi-flow vector to the injection vector.

Lemma 1 *Consider two arbitrary injection vectors $\bar{\mathbf{p}}_n$ and $\tilde{\mathbf{p}}_n$ in $\mathcal{P}$, associated with the semi-flow vectors $\bar{\mathbf{p}}_d$ and $\tilde{\mathbf{p}}_d$ (defined in (2)). The relation*

$$\bar{\mathbf{p}}_n - \tilde{\mathbf{p}}_n = M(\bar{\mathbf{p}}_d, \tilde{\mathbf{p}}_d) \times (\bar{\mathbf{p}}_d - \tilde{\mathbf{p}}_d) \tag{13}$$

holds.

Proof: One can write

$$\bar{p}_i - \tilde{p}_i = \sum_{j \in \mathcal{N}(i)} (\bar{p}_{ij} - \tilde{p}_{ij}), \qquad \forall i \in \mathcal{N} \tag{14}$$

By using the relations

$$\bar{p}_{ji} = f_{ij}(\bar{p}_{ij}), \quad \tilde{p}_{ji} = f_{ij}(\tilde{p}_{ij}), \quad \forall (i,j) \in \overrightarrow{\mathcal{E}} \tag{15}$$

it is straightforward to verify that (13) and (14) are equivalent. ■

Lemma 1 can be regarded as a generalization of the conventional node-edge adjacency matrix used to describe the topology of the graph, which relates semi-flow vectors to injection vectors. The next lemma investigates an important property of the matrix $M(\bar{\mathbf{p}}_d, \tilde{\mathbf{p}}_d)$.

Lemma 2 *Given two arbitrary points $\bar{\mathbf{p}}_d, \tilde{\mathbf{p}}_d \in \mathcal{B}_d$, assume that there exists a nonzero vector $\mathbf{x} \in \mathbb{R}^m$ such that $\mathbf{x}^T M(\bar{\mathbf{p}}_d, \tilde{\mathbf{p}}_d) \geq 0$. If $\mathbf{x}$ has at least one strictly positive entry, then there exists a nonzero vector $\mathbf{y} \in \mathbb{R}^m_+$ such that $\mathbf{y}^T M(\bar{\mathbf{p}}_d, \tilde{\mathbf{p}}_d) \geq 0$.*

Proof: Consider an index $i_0 \in \mathcal{N}$ such that $x_{i_0} > 0$. Define $\mathcal{V}(i_0)$ as the set of all vertices $i \in \mathcal{N}$ from which there exists a directed path to vertex i_0 in the graph $\overrightarrow{\mathcal{G}}$. Note that $\mathcal{V}(i_0)$ includes vertex i_0 itself. The first goal is to show that

$$x_i \geq 0, \qquad \forall i \in \mathcal{V}(i_0) \tag{16}$$

To this end, consider an arbitrary set of vertices $i_1, ..., i_k$ in $\mathcal{V}(i_0)$ such that $\{i_0, i_1 ..., i_k\}$ forms a direct path in $\overrightarrow{\mathcal{G}}$ as

$$i_k \to i_{k-1} \to \cdots i_1 \to i_0 \tag{17}$$

To prove (16), it suffices to show that $x_{i_1}, ..., x_{i_k} \geq 0$. For this purpose, one can expand the product $\mathbf{x}^T M(\bar{\mathbf{p}}_d, \tilde{\mathbf{p}}_d)$ and use the fact that each column of $M(\bar{\mathbf{p}}_d, \tilde{\mathbf{p}}_d)$ has $m-2$ zero entries to conclude that

$$x_{i_1} + \frac{f_{i_1 i_0}(\bar{p}_{i_1 i_0}) - f_{i_1 i_0}(\tilde{p}_{i_1 i_0})}{\bar{p}_{i_1 i_0} - \tilde{p}_{i_1 i_0}} x_{i_0} \geq 0 \tag{18}$$

Since x_{i_0} is positive and $f_{i_1 i_0}(\cdot)$ is a decreasing function, x_{i_1} turns out to be positive. Now, repeating the above argument for i_1 instead of i_0 yields that $x_{i_2} \geq 0$. Continuing this reasoning leads to $x_{i_1}, ..., x_{i_k} \geq 0$. Hence, inequality (16) holds. Now, define $\mathbf{y}$ as

$$y_i = \begin{cases} x_i & \text{if} \quad i \in \mathcal{V}(i_0) \\ 0 & \text{otherwise} \end{cases}, \qquad \forall i \in \mathcal{N} \tag{19}$$

In light of (16), $\mathbf{y}$ is a nonzero vector in $\mathbb{R}^m_+$. To complete the proof, it suffices to show that $\mathbf{y}^T M(\bar{\mathbf{p}}_d, \tilde{\mathbf{p}}_d) \geq 0$. Similar to the indexing procedure used for the columns of the matrix $M(\bar{\mathbf{p}}_d, \tilde{\mathbf{p}}_d)$, we index the entries of the $|\overrightarrow{\mathcal{E}}|$ dimensional vector $\mathbf{y}^T M(\bar{\mathbf{p}}_d, \tilde{\mathbf{p}}_d)$ according to the edges of $\overrightarrow{\mathcal{G}}$. Now, given an arbitrary edge $(\alpha, \beta) \in \overrightarrow{\mathcal{E}}$, the following statements hold true:

- If $\alpha, \beta \in \mathcal{V}(i_0)$, then the $(\alpha, \beta)^{\text{th}}$ entries of $\mathbf{y}^T M(\bar{\mathbf{p}}_d, \tilde{\mathbf{p}}_d)$ and $\mathbf{x}^T M(\bar{\mathbf{p}}_d, \tilde{\mathbf{p}}_d)$ (i.e., the entries corresponding to the edge (α, β)) are identical.
- If $\alpha \in \mathcal{V}(i_0)$ and $\beta \notin \mathcal{V}(i_0)$, then the $(\alpha, \beta)^{\text{th}}$ entry of $\mathbf{y}^T M(\bar{\mathbf{p}}_d, \tilde{\mathbf{p}}_d)$ is equal to y_α.
- If $\alpha \notin \mathcal{V}(i_0)$ and $\beta \notin \mathcal{V}(i_0)$, then the $(\alpha, \beta)^{\text{th}}$ entry of $\mathbf{y}^T M(\bar{\mathbf{p}}_d, \tilde{\mathbf{p}}_d)$ is equal to zero.

Note that the case $\alpha \notin \mathcal{V}(i_0)$ and $\beta \in \mathcal{V}(i_0)$ cannot happen, because if $\beta \in \mathcal{V}(i_0)$ and $(\alpha, \beta) \in \overrightarrow{\mathcal{E}}$, then $\alpha \in \mathcal{V}(i_0)$ by the definition of $\mathcal{V}(i_0)$. It follows from the above results and the inequality $\mathbf{x}^T M(\bar{\mathbf{p}}_d, \tilde{\mathbf{p}}_d) \geq 0$ that $\mathbf{y}^T M(\bar{\mathbf{p}}_d, \tilde{\mathbf{p}}_d) \geq 0$. ■

Definition 7 *Consider the graph $\mathcal{G}$ and an arbitrary flow vector $\mathbf{p}_e$. Given a subgraph $\mathcal{G}_s$ of the graph $\mathcal{G}$, define $\mathbf{p}_e(\mathcal{G}_s)$ as the flow vector associated with the edges of $\mathcal{G}_s$ that has been induced by $\mathbf{p}_e$. Define $\mathbf{p}_d(\mathcal{G}_s)$, $\mathbf{p}_n(\mathcal{G}_s)$ and $p_i(\mathcal{G}_s)$ as the semi-flow vector, injection vector and injection at node $i \in \mathcal{G}_s$ corresponding to $\mathbf{p}_e(\mathcal{G}_s)$, respectively. Define also $\mathcal{P}(\mathcal{G}_s)$ as the injection region associated with $\mathcal{G}_s$.*

The next lemma studies the injection region $\mathcal{P}$ in the case where $f_{ij}(\cdot)$'s are all piecewise linear.

Lemma 3 *Assume that the function $f_{ij}(\cdot)$ is piecewise linear for every $(i, j) \in \overrightarrow{\mathcal{E}}$. Consider two arbitrary points $\hat{\mathbf{p}}_n, \bar{\mathbf{p}}_n \in \mathcal{P}$ and a vector $\Delta\bar{\mathbf{p}}_n \in \mathbb{R}^m$ satisfying the relations*

$$\hat{\mathbf{p}}_n \leq \bar{\mathbf{p}}_n - \Delta\bar{\mathbf{p}}_n \leq \bar{\mathbf{p}}_n \tag{20}$$

There exists a strictly positive number ϵ^{max} with the property

$$\bar{\mathbf{p}}_n - \varepsilon\Delta\bar{\mathbf{p}}_n \in \mathcal{P}, \qquad \forall \varepsilon \in [0, \epsilon^{max}] \tag{21}$$

Proof: In light of (20), we have $\Delta\bar{\mathbf{p}}_n \geq 0$. If $\Delta\bar{\mathbf{p}}_n = 0$, then the lemma becomes trivial as ε can take any arbitrary value. So, assume that $\Delta\bar{\mathbf{p}}_n \neq 0$. Let $\hat{\mathbf{p}}_e$ and $\bar{\mathbf{p}}_e$ denote two flow vectors associated with the injection vectors $\hat{\mathbf{p}}_n$ and $\bar{\mathbf{p}}_n$, respectively. Denote the corresponding semi-flow vectors as $\hat{\mathbf{p}}_d$ and $\bar{\mathbf{p}}_d$. Given an edge $(i, j) \in \overrightarrow{\mathcal{E}}$, the curve

$$\big\{(p_{ij}, f_{ij}(p_{ij})) \mid p_{ij} \in [p_{ij}^{\min}, p_{ij}^{\max}]\big\} \tag{22}$$

is a Pareto set in $\mathbb{R}^2$ due to $f_{ij}(\cdot)$ being monotonically decreasing. Since $(\hat{p}_{ij}, \hat{p}_{ji})$ and $(\bar{p}_{ij}, \bar{p}_{ji})$ both lie on the above curve, one of the following cases occurs:

- *Case 1:* $\hat{p}_{ij} \geq \bar{p}_{ij}$ and $\hat{p}_{ji} \leq \bar{p}_{ji}$.

– *Case 2:* $\hat{p}_{ij} \le \bar{p}_{ij}$ and $\hat{p}_{ji} \ge \bar{p}_{ji}$.

(this fact can be observed in Figure 4(c) for the points $(\bar{p}_{ij}, \bar{p}_{ji})$ and $(\tilde{p}_{ij}, \tilde{p}_{ji})$ instead of $(\hat{p}_{ij}, \hat{p}_{ji})$ and $(\bar{p}_{ij}, \bar{p}_{ji})$). With no loss of generality, assume that Case 1 occurs. Indeed, if Case 2 happens, it suffices to make two changes:

– Change the orientation of the edge (i, j) in the graph $\overrightarrow{\mathcal{G}}$ so that $(j, i) \in \overrightarrow{\mathcal{E}}$ instead of $(i, j) \in \overrightarrow{\mathcal{E}}$.
– Replace the constraint $p_{ji} = f_{ij}(p_{ij})$ in (4c) with $p_{ij} = f_{ij}^{-1}(p_{ji})$, where the existence, monotonicity and convexity of the inverse function $f_{ij}^{-1}(\cdot)$ is guaranteed by the convexity and decreasing property of $f_{ij}(\cdot)$.

Therefore, suppose that

$$\hat{p}_{ij} \ge \bar{p}_{ij}, \quad \hat{p}_{ji} \le \bar{p}_{ji}, \qquad \forall (i, j) \in \overrightarrow{\mathcal{E}} \tag{23}$$

or

$$\hat{\mathbf{p}}_d \ge \bar{\mathbf{p}}_d \tag{24}$$

First, consider the case $\hat{\mathbf{p}}_d > \bar{\mathbf{p}}_d$. In light of Lemma 1, the assumption $\hat{\mathbf{p}}_n \le \bar{\mathbf{p}}_n$ can be expressed as

$$M(\hat{\mathbf{p}}_d, \bar{\mathbf{p}}_d) \times (\hat{\mathbf{p}}_d - \bar{\mathbf{p}}_d) = \hat{\mathbf{p}}_n - \bar{\mathbf{p}}_n \le 0 \tag{25}$$

In order to guarantee the relation $\bar{\mathbf{p}}_n - \varepsilon \Delta \bar{\mathbf{p}}_n \in \mathcal{P}$, it suffices to seek a vector $\Delta \bar{\mathbf{p}}_d \in \mathbb{R}^{|\overrightarrow{\mathcal{E}}|}$ satisfying the equations

$$\bar{\mathbf{p}}_d - \varepsilon \Delta \bar{\mathbf{p}}_d \in \mathcal{B}_d \tag{26}$$

and

$$M(\bar{\mathbf{p}}_d, \bar{\mathbf{p}}_d - \varepsilon \Delta \bar{\mathbf{p}}_d) \times (\bar{\mathbf{p}}_d - (\bar{\mathbf{p}}_d - \varepsilon \Delta \bar{\mathbf{p}}_d)) = \bar{\mathbf{p}}_n - (\bar{\mathbf{p}}_n - \varepsilon \Delta \bar{\mathbf{p}}_n) \tag{27}$$

(see the proof of Lemma 1), or equivalently

$$\bar{\mathbf{p}}_d - \varepsilon \Delta \bar{\mathbf{p}}_d \in \mathcal{B}_d \tag{28a}$$
$$M(\bar{\mathbf{p}}_d, \bar{\mathbf{p}}_d - \varepsilon \Delta \bar{\mathbf{p}}_d) \times \Delta \bar{\mathbf{p}}_d = \Delta \bar{\mathbf{p}}_n \tag{28b}$$

Consider an arbitrary vector $\Delta \bar{\mathbf{p}}_d \in \mathbb{R}^{|\overrightarrow{\mathcal{E}}|}$ with all negative entries. In light of Definition 6, the inequality $\hat{\mathbf{p}}_d > \bar{\mathbf{p}}_d$ and the piecewise linear property of $f_{ij}(\cdot)$'s, there exists a positive number $\varepsilon^{\max}$ such that

$$\bar{\mathbf{p}}_d - \varepsilon \Delta \bar{\mathbf{p}}_d \in \mathcal{B}_d \tag{29a}$$
$$M(\bar{\mathbf{p}}_d, \bar{\mathbf{p}}_d - \varepsilon \Delta \bar{\mathbf{p}}_d) = M(\bar{\mathbf{p}}_d, \bar{\mathbf{p}}_d) \tag{29b}$$

for every $\varepsilon \in [0, \varepsilon^{\max}]$. To prove the lemma, it follows from (28) and (29) that it is enough to show the existence of a negative vector $\Delta \bar{\mathbf{p}}_d$ satisfying the relation

$$M(\bar{\mathbf{p}}_d, \bar{\mathbf{p}}_d) \times \Delta \bar{\mathbf{p}}_d = \Delta \bar{\mathbf{p}}_n \tag{30}$$

in which ε does not appear. Notice that since (30) is independent of ϵ, it can be chosen sufficiently small so that (29a) is satisfied automatically. To prove this by contradiction, assume that the above equation does not have a solution. By Farkas' Lemma, there exists a vector $\mathbf{x} \in \mathbb{R}^m$ such that

$$\mathbf{x}^T M(\bar{\mathbf{p}}_d, \bar{\mathbf{p}}_d) \geq 0, \qquad \mathbf{x}^T \Delta\bar{\mathbf{p}}_n > 0 \tag{31}$$

Since $\Delta\bar{\mathbf{p}}_n$ is nonnegative, the inequality $\mathbf{x}^T \Delta\bar{\mathbf{p}}_n > 0$ does not hold unless $\mathbf{x}$ has at least one strictly positive entry. Now, it follows from $\mathbf{x}^T M(\bar{\mathbf{p}}_d, \bar{\mathbf{p}}_d) \geq 0$ and Lemma 2 that there exists a nonzero vector $\mathbf{y} \in \mathbb{R}^m$ such that

$$\mathbf{y}^T M(\bar{\mathbf{p}}_d, \bar{\mathbf{p}}_d) \geq 0, \qquad \mathbf{y} \geq 0 \tag{32}$$

On the other hand, given an edge $(i,j) \in \overrightarrow{\mathcal{E}}$, since $\hat{p}_{ij} \geq \bar{p}_{ij}$ (due to (23)), the slope of the line connecting the points $(\hat{p}_{ij}, \hat{p}_{ji})$ and $(\bar{p}_{ij}, \bar{p}_{ji})$ is more than or equal to $f'_{ij}(\bar{p}_{ij})$ (this is implied by the fact that $f_{ij}(\cdot)$ is convex). This yields that

$$M(\bar{\mathbf{p}}_d, \bar{\mathbf{p}}_d) \leq M(\hat{\mathbf{p}}_d, \bar{\mathbf{p}}_d) \tag{33}$$

Now, it follows from (24), (25), (32) and (33) that

$$0 \geq \mathbf{y}^T M(\hat{\mathbf{p}}_d, \bar{\mathbf{p}}_d) \times (\hat{\mathbf{p}}_d - \bar{\mathbf{p}}_d) \geq \mathbf{y}^T M(\bar{\mathbf{p}}_d, \bar{\mathbf{p}}_d) \times (\hat{\mathbf{p}}_d - \bar{\mathbf{p}}_d) \geq 0 \tag{34}$$

Thus,

$$0 = \mathbf{y}^T M(\hat{\mathbf{p}}_d, \bar{\mathbf{p}}_d) \times (\hat{\mathbf{p}}_d - \bar{\mathbf{p}}_d) = \mathbf{y}^T (\hat{\mathbf{p}}_n - \bar{\mathbf{p}}_n) \tag{35}$$

This is a contradiction because $\hat{\mathbf{p}}_n - \bar{\mathbf{p}}_n$ is strictly negative and the nonzero vector $\mathbf{y}$ is positive.

So far, the lemma has been proven in the case when $\hat{\mathbf{p}}_d > \bar{\mathbf{p}}_d$. To extend the proof to the case $\hat{\mathbf{p}}_d \geq \bar{\mathbf{p}}_d$, define $\mathcal{E}_\mathrm{r}$ as the set of every edge $(i,j) \in \mathcal{E}$ such that

$$\hat{p}_{ij} \neq \bar{p}_{ij} \tag{36}$$

(note that $\hat{p}_{ij} = \bar{p}_{ij}$ if and only if $\hat{p}_{ji} = \bar{p}_{ji}$). Define also $\mathcal{G}_\mathrm{r}$ as the unique subgraph of $\mathcal{G}$ induced by the edge set $\mathcal{E}_\mathrm{r}$. Let $\mathcal{N}_\mathrm{r}$ denote the vertex set of $\mathcal{G}_\mathrm{r}$, which may be different from $\mathcal{N}$. It is easy to verify that

$$\hat{\mathbf{p}}_d(\mathcal{G}_\mathrm{r}) > \bar{\mathbf{p}}_d(\mathcal{G}_\mathrm{r}), \tag{37a}$$

$$\hat{\mathbf{p}}_n(\mathcal{G}_\mathrm{r}) \leq \bar{\mathbf{p}}_n(\mathcal{G}_\mathrm{r}) - \Delta\bar{\mathbf{p}}_n(\mathcal{G}_\mathrm{r}) \leq \bar{\mathbf{p}}_n(\mathcal{G}_\mathrm{r}) \tag{37b}$$

$$\bar{p}_i - \hat{p}_i = \bar{p}_i(\mathcal{G}_\mathrm{r}) - \hat{p}_i(\mathcal{G}_\mathrm{r}), \qquad \forall i \in \mathcal{N}_\mathrm{r} \tag{37c}$$

Based on (37c), the relationship between $\Delta\bar{\mathbf{p}}_n$ and the new vector $\Delta\bar{\mathbf{p}}_n(\mathcal{G}_\mathrm{r})$ is as follows:

$$\Delta\bar{p}_i = \begin{cases} \Delta\bar{p}_i(\mathcal{G}_\mathrm{r}) & \text{if} \quad i \in \mathcal{N}_\mathrm{r} \\ 0 & \text{otherwise} \end{cases}, \qquad \forall i \in \mathcal{N} \tag{38}$$

In light of (37a) and (37b), one can adopt the proof given earlier for the case $\hat{\mathbf{p}}_d > \bar{\mathbf{p}}_d$ to conclude the existence of a positive number $\epsilon^{\max}$ with the property

$$\bar{\mathbf{p}}_n(\mathcal{G}_\mathrm{r}) - \varepsilon\Delta\bar{\mathbf{p}}_n(\mathcal{G}_\mathrm{r}) \in \mathcal{P}(\mathcal{G}_\mathrm{r}), \qquad \forall \varepsilon \in [0, \epsilon^{\max}] \tag{39}$$

Given an arbitrary number $\varepsilon \in [0, \epsilon^{\max}]$, we use the shorthand notation $\mathbf{p}_n(\mathcal{G}_{\rm r})$ and $\mathbf{p}_n$ for $\bar{\mathbf{p}}_n(\mathcal{G}_{\rm r}) - \varepsilon \Delta\bar{\mathbf{p}}_n(\mathcal{G}_{\rm r})$ and $\bar{\mathbf{p}}_n - \varepsilon\Delta\bar{\mathbf{p}}_n$, respectively. Let $\mathbf{p}_e(\mathcal{G}_{\rm r})$ and $\mathbf{p}_e$ denote a flow vector corresponding to the injection vectors $\mathbf{p}_n(\mathcal{G}_{\rm r})$ and $\mathbf{p}_n$, respectively. One can expand the vector $\mathbf{p}_e(\mathcal{G}_{\rm r})$ into $\mathbf{p}_e$ for the graph $\mathcal{G}$ as follows:

- For every $(i,j) \in \mathcal{E}_{\rm r}$, the $(i,j)^{\rm th}$ entries of $\mathbf{p}_e$ and $\mathbf{p}_e(\mathcal{G}_{\rm r})$ (the ones corresponding to the edge (i,j)) are identical.
- For every $(i,j) \in \mathcal{E}\backslash\mathcal{E}_{\rm r}$, the $(i,j)^{\rm th}$ entry of $\mathbf{p}_e$ is equal to $\bar{p}_{ij}$ (or $\hat{p}_{ij}$).

It is straightforward to observe that $\mathbf{p}_n$ is associated with the designed vector $\mathbf{p}_e$ and, therefore, the feasibility of $\mathbf{p}_e$ implies that $\mathbf{p}_n$ belongs to $\mathcal{P}$. This completes the proof. ■

The next lemma uses Lemma 3 to prove Theorem 1 in the case where $f_{ij}(\cdot)$'s are all piecewise linear.

Lemma 4 *Assume that the function $f_{ij}(\cdot)$ is piecewise linear for every $(i,j) \in \overrightarrow{\mathcal{E}}$. Given any two arbitrary points $\hat{\mathbf{p}}_n, \tilde{\mathbf{p}}_n \in \mathcal{P}$, the box $\mathcal{B}(\hat{\mathbf{p}}_n, \tilde{\mathbf{p}}_n)$ is a subset of the injection region $\mathcal{P}$.*

Proof: With no loss of generality, assume that $\hat{\mathbf{p}}_n \leq \tilde{\mathbf{p}}_n$ (because otherwise $\mathcal{B}(\hat{\mathbf{p}}_n, \tilde{\mathbf{p}}_n)$ is empty). To prove the lemma by contradiction, suppose that there exists a point $\mathbf{p}_n \in \mathcal{B}(\hat{\mathbf{p}}_n, \tilde{\mathbf{p}}_n)$ such that $\mathbf{p}_n \notin \mathcal{P}$. Consider the set

$$\left\{ \gamma \;\middle|\; \gamma \in [0,1],\ \tilde{\mathbf{p}}_n + \gamma(\mathbf{p}_n - \tilde{\mathbf{p}}_n) \in \mathcal{P} \right\} \tag{40}$$

Note that $\hat{\mathbf{p}}_n \leq \mathbf{p}_n \leq \tilde{\mathbf{p}}_n$, and that (40) describes the set of all γ's for which $\tilde{\mathbf{p}}_n + \gamma(\mathbf{p}_n - \tilde{\mathbf{p}}_n)$ belongs to the segment between $\mathbf{p}_n$ and $\tilde{\mathbf{p}}_n$. Denote the maximum of all those γ as $\gamma^{\max}$. The existence of this number is guaranteed because of two reasons: (1) when γ is equal to 0, the point $\tilde{\mathbf{p}}_n + \gamma(\mathbf{p}_n - \tilde{\mathbf{p}}_n)$ is equal to $\tilde{\mathbf{p}}_n$ and belongs to $\mathcal{P}$, (2) $\mathcal{P}$ is closed and compact. Furthermore, notice that $\tilde{\mathbf{p}}_n + \gamma(\mathbf{p}_n - \tilde{\mathbf{p}}_n)$ is equal to $\mathbf{p}_n$ at $\gamma = 1$. Since $\mathbf{p}_n \notin \mathcal{P}$ by assumption, we have $\gamma^{\max} < 1$. Denote $\tilde{\mathbf{p}}_n + \gamma^{\max}(\mathbf{p}_n - \tilde{\mathbf{p}}_n)$ as $\bar{\mathbf{p}}_n$. Hence, $\bar{\mathbf{p}}_n \in \mathcal{P}$ and $\hat{\mathbf{p}}_n \leq \mathbf{p}_n \leq \bar{\mathbf{p}}_n$ (recall that $\gamma^{\max} < 1$). Define $\Delta\bar{\mathbf{p}}_n$ as $\bar{\mathbf{p}}_n - \mathbf{p}_n$. One can write:

$$\hat{\mathbf{p}}_n \leq \bar{\mathbf{p}}_n - \Delta\bar{\mathbf{p}}_n \leq \bar{\mathbf{p}}_n, \qquad \hat{\mathbf{p}}_n, \bar{\mathbf{p}}_n \in \mathcal{P} \tag{41}$$

By Lemma 3, there exists a strictly positive number $\epsilon^{\max}$ with the property

$$\bar{\mathbf{p}}_n - \varepsilon\Delta\bar{\mathbf{p}}_n \in \mathcal{P}, \qquad \forall \varepsilon \in [0, \epsilon^{\max}] \tag{42}$$

or equivalently

$$\tilde{\mathbf{p}}_n + (\gamma^{\max} + \varepsilon(1 - \gamma^{\max}))(\mathbf{p}_n - \tilde{\mathbf{p}}_n) \in \mathcal{P}, \quad \forall \varepsilon \in [0, \epsilon^{\max}] \tag{43}$$

Notice that

$$\gamma^{\max} + \varepsilon(1 - \gamma^{\max}) > \gamma^{\max}, \quad \forall \varepsilon > 0 \tag{44}$$

Due to (43), this violates the assumption that $\gamma^{\max}$ is the maximum of the set given in (40). ■

Lemma 4 will be deployed next to prove Theorem 1 in the general case.

Proof of Theorem 1: Consider an arbitrary approximation of $f_{ij}(\cdot)$ by a piecewise linear function for every $(i,j) \in \mathcal{E}$. As a counterpart of $\mathcal{P}$, let $\mathcal{P}_s$ denote the injection region in the piecewise-linear case. By Lemma 4, we have

$$\mathcal{B}(\hat{\mathbf{p}}_n, \tilde{\mathbf{p}}_n) \subseteq \mathcal{P}_s \tag{45}$$

Since the piecewise linear approximation can be made in such a way that the sets $\mathcal{P}$ and $\mathcal{P}_s$ become arbitrarily close to each other, the above relation implies that the interior of $\mathcal{B}(\hat{\mathbf{p}}_n, \tilde{\mathbf{p}}_n)$ is a subset of $\mathcal{P}$. On the other hand, $\mathcal{P}$ is a closed set. Hence, the box $\mathcal{B}(\hat{\mathbf{p}}_n, \tilde{\mathbf{p}}_n)$ must entirely belong to $\mathcal{P}$. ■

3.3 Relationship Between GNF and CGNF

Using Theorem 1 developed in the preceding subsection, we study the relationship between GNF and CGNF below.

Definition 8 *Consider an arbitrary set $\mathcal{S} \in \mathbb{R}^n$ together with a point $\mathbf{x} \in \mathcal{S}$. The point $\mathbf{x}$ is called "Pareto" if there does not exist another point $\mathbf{y} \in \mathcal{S}$ that is less than or equal to $\mathbf{x}$ entry-wise. $\mathbf{x} \in \mathcal{S}$ is called an "interior point" if $\mathcal{S}$ contains a ball around this point. $\mathbf{x} \in \mathcal{S}$ is called a "boundary point" if it is not an interior point.*

To proceed with the paper, the following mild assumption is required.

Assumption 1 *There exists a feasible point $(\mathbf{p}_n, \mathbf{p}_e)$ for the CGNF problem such that $p_{ij} > p_{ij}^{min}$ for every $(i,j) \in \overrightarrow{\mathcal{E}}$ and $p_i < p_i^{max}$ for every $i \in \mathcal{N}$.*

Theorem 2 *Assume that the GNF problem is feasible. Let $(\mathbf{p}_n^*, \mathbf{p}_e^*)$ and $(\bar{\mathbf{p}}_n^*, \bar{\mathbf{p}}_e^*)$ denote arbitrary globally optimal solutions of GNF and CGNF, respectively. The following relations hold:*

1) $\mathbf{p}_n^* = \bar{\mathbf{p}}_n^*$
2) $(\bar{\mathbf{p}}_n^*, \bar{\mathbf{p}}_e^*)$ *is a solution of GNF, provided that* $\mathbf{p}_n^*$ *is a Pareto point in* $\mathcal{P}$.

■

In what follows, we first prove Part 2 of Theorem 2 and illustrate it in some examples before proving Part 1.

Proof of Part 2 of Theorem 2: Define a new flow vector $\hat{\mathbf{p}}_e$ as

$$\hat{p}_{ij} = \bar{p}_{ij}^*, \qquad \forall (i,j) \in \overrightarrow{\mathcal{E}} \tag{46a}$$

$$\hat{p}_{ji} = f_{ij}(\bar{p}_{ij}^*), \qquad \forall (i,j) \in \overrightarrow{\mathcal{E}} \tag{46b}$$

Let $\hat{\mathbf{p}}_n$ denote the injection vector corresponding to $\hat{\mathbf{p}}_e$. Since $\hat{p}_{ji} = f_{ij}(\bar{p}_{ij}^*)$ for every $(i,j) \in \overrightarrow{\mathcal{E}}$, it can be concluded that $\hat{\mathbf{p}}_n \leq \bar{\mathbf{p}}_n^* = \mathbf{p}_n^*$ (the last equality follows from Part 1 of the theorem). Since $\mathbf{p}_n^*$ is assumed to be a Pareto point

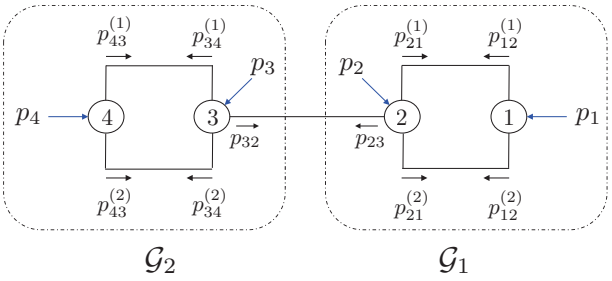

Fig. 5: The 4-node graph $\mathcal{G}$ studied in Example 2.

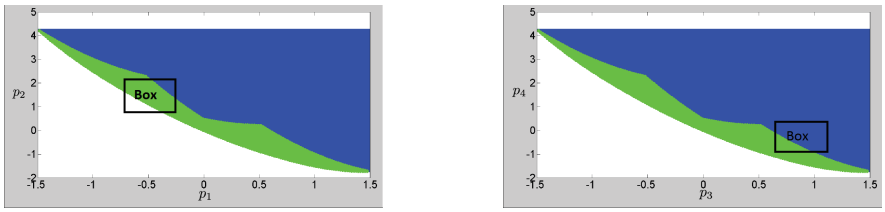

(a) (b)

Fig. 6: (a) Injection region of the subgraph $\mathcal{G}_1$ in Example 2; (b): injection region of the subgraph $\mathcal{G}_2$ in Example 2.

in $\mathcal{P}$, we must have $\hat{\mathbf{p}}_n = \bar{\mathbf{p}}_n^*$ and therefore $\hat{\mathbf{p}}_e = \bar{\mathbf{p}}_e^*$. This implies that $(\bar{\mathbf{p}}_n^*, \bar{\mathbf{p}}_e^*)$ is a feasible point for GNF and yet a global solution for CGNF. As a result, $(\bar{\mathbf{p}}_n^*, \bar{\mathbf{p}}_e^*)$ is a solution of GNF. ■

Theorem 2 states that CGNF finds the optimal injections but not necessarily optimal flows for GNF. Note that Part 1 of the theorem implies that the globally optimal injection vector is unique. Two examples will be provided below to elaborate on Part 2 of Theorem 2.

Example 1: Consider the illustrative example explained in Section 3.1. It can be observed in Figure 2(b) that every point on the lower curvy boundary of the feasible set is a Pareto point. Therefore, if the box $\mathcal{B}$ defined by the lower and upper bound constraints on p_1 and p_2 intersects with any part of the lower boundary of the green area, CGNF always finds optimal flow vectors for GNF, leading to the equivalence of GNF and CGNF. ■

Example 2: As stated before, a Pareto point lies on the boundary of the injection region. A question arises as to whether the condition "Pareto point" can be replaced by "boundary point" in Theorem 2. We will provide an example here to show that the optimal injection being a boundary point does not necessarily guarantee the equivalence of GNF and CGNF. To this end, consider the 4-node graph $\mathcal{G}$ depicted in Figure 5. This graph can be decomposed into two subgraphs $\mathcal{G}_1$ and $\mathcal{G}_2$, where each subgraph has the same

topology as the 2-node graph studied in Example 1. Assume that the flow over the line $(2,3)$ is restricted to zero, by imposing the constraints $p_{23}^{\min} = p_{23}^{\max} = p_{32}^{\min} = p_{32}^{\max} = 0$. This implies that $(2,3)$ is redundant, whose removal splits the graph $\mathcal{G}$ into two disjoint subgraphs $\mathcal{G}_1$ and $\mathcal{G}_2$. Let $(\mathbf{p}_n^*, \mathbf{p}_e^*)$ be an arbitrary solution of GNF. The vector $\mathbf{p}_n^*$ can be broken down into two parts as

$$\mathbf{p}_n^* = [\mathbf{p}_n^*(\mathcal{G}_1)^T \quad \mathbf{p}_n^*(\mathcal{G}_2)^T]^T \tag{47}$$

where $\mathbf{p}_n^*(\mathcal{G}_1)$ and $\mathbf{p}_n^*(\mathcal{G}_2)$ denote the optimal values of the sub-vectors $[p_1 \;\; p_2]^T$ and $[p_3 \;\; p_4]^T$, respectively. Note that $\mathcal{P}(\mathcal{G}_1)$ and $\mathcal{P}(\mathcal{G}_2)$ could both resemble the green area in Figure 2(b). We make two assumptions here:

- *Assumption 1:* As demonstrated in Figure 6(a), the box constraints on p_1 and p_2 are such that $\mathbf{p}_n^*(\mathcal{G}_1)$ becomes a Pareto point located on the lower boundary of $\mathcal{P}(\mathcal{G}_1)$. In this case, it is guaranteed from Theorem 2 that if CGNF is solved just over $\mathcal{G}_1$, it finds feasible flows for this subgraph.
- *Assumption 2:* As demonstrated in Figure 6(b), the box constraints on p_3 and p_4 are such that $\mathbf{p}_n^*(\mathcal{G}_2)$ becomes an interior point of $\mathcal{P}(\mathcal{G}_2)$, corresponding to the lower left corner of the box. In this case, assume that if CGNF is solved just over $\mathcal{G}_2$, it may not always find feasible flows for this subgraph (we will show it later in the paper).

Since $(2,3)$ is not allowed to carry any flow, it is easy to show that CGNF solved over $\mathcal{G}$ finds feasible flows for the lines between nodes 1 and 2, but may result in wrong flows for the lines between nodes 3 and 4. Hence, CGNF and GNF are not equivalent. On the other hand, it is straightforward to inspect that $\mathcal{P}$ is the product of two regions as

$$\mathcal{P} = \mathcal{P}(\mathcal{G}_1) \times \mathcal{P}(\mathcal{G}_2) \tag{48}$$

Now, since $\mathbf{p}_n^*(\mathcal{G}_1)$ is on the boundary of $\mathcal{P}(\mathcal{G}_1)$ but $\mathbf{p}_n^*(\mathcal{G}_2)$ is in the interior of $\mathcal{P}(\mathcal{G}_2)$, it can be deduced that

- $\mathbf{p}_n^*$ is on the boundary of the injection region $\mathcal{P}$.
- $\mathbf{p}_n^*$ is not a Pareto point of the injection region $\mathcal{P}$.

In summary, although $\mathbf{p}_n^*$ is a boundary point for $\mathcal{G}$, CGNF is not equivalent to GNF. This is due to the connection of a well-behaved subgraph $\mathcal{G}_1$ to a problematic subgraph $\mathcal{G}_2$ via a redundant link with no flow. It will be shown in Corollary 2 that whenever $\mathbf{p}_n^*$ is on the boundary of its injection region, there exists a non-empty subgraph of $\mathcal{G}$ for which the correct (feasible and optimal) flows can be found via CGNF. ■

Before presenting the proof of Part 1 of Theorem 2 in the general case, one special case will be studied for which the proof is less involved. Observe that since $(\bar{\mathbf{p}}_n^*, \bar{\mathbf{p}}_e^*)$ is a feasible point of CGNF, one can write

$$\bar{p}_i^* \geq p_i^{\min}, \qquad \forall i \in \mathcal{N} \tag{49}$$

The proof of Part 1 of Theorem 2 will be first derived in the special case

$$\bar{p}_i^* = p_i^{\min}, \qquad \forall i \in \mathcal{N} \tag{50}$$

Proof of Part 1 of Theorem 2 under Condition (50): $(\mathbf{p}_n^*, \mathbf{p}_e^*)$ being a feasible point of GNF implies that

$$p_i^* \geq p_i^{\min}, \qquad \forall i \in \mathcal{N} \tag{51}$$

Equations (50) and (51) lead to

$$\bar{\mathbf{p}}_n^* \leq \mathbf{p}_n^* \tag{52}$$

Define the vector $\tilde{\mathbf{p}}_n$ as

$$\tilde{p}_i = \sum_{(i,j)\in\overrightarrow{\mathcal{E}}} \bar{p}_{ij}^* + \sum_{(j,i)\in\overrightarrow{\mathcal{E}}} f_{ij}(\bar{p}_{ij}^*), \qquad \forall i \in \mathcal{N} \tag{53}$$

Notice that $\tilde{\mathbf{p}}_n$ belongs to $\mathcal{P}$, although it may not belong to $\mathcal{B}$. It can be inferred from the definition of CGNF that

$$\tilde{\mathbf{p}}_n \leq \bar{\mathbf{p}}_n^* \tag{54}$$

Since $\tilde{\mathbf{p}}_n, \mathbf{p}_n^* \in \mathcal{P}$, it follows from Theorem 1, (52) and (54) that $\bar{\mathbf{p}}_n^* \in \mathcal{P}$. On the other hand, $\bar{\mathbf{p}}_n^* \in \mathcal{B}$. Therefore, $\bar{\mathbf{p}}_n^* \in \mathcal{P} \cap \mathcal{B}$, implying that $\bar{\mathbf{p}}_n^*$ is a feasible point of Geometric GNF. Since the feasible set of Geometric CGNF includes that of Geometric GNF, $\bar{\mathbf{p}}_n^*$ must be a solution of Geometric GNF as well. The proof follows from equation (52) and the fact that $\mathbf{p}_n^*$ is another solution of Geometric GNF (recall that the objective function of this optimization problem is strictly increasing). ■

Before proving Part 1 of Theorem 2 in the general case, some ideas need to be developed. Since $f_i(p_i)$ can be approximated by a differentiable function arbitrarily precisely, with no loss of generality, assume that $f_i(p_i)$ is differentiable for every $i \in \mathcal{N}$. Since CGNF is convex, one can take its Lagrangian dual.

Lemma 5 *Strong duality holds for the CGNF problem.*

Proof: To prove the lemma, it suffices to show that Slater's condition is satisfied or, alternatively, there exists a feasible solution for the CGNF problem satisfying (6c) with strict inequality. To this end, consider the feasible solution $(\mathbf{p}_n, \mathbf{p}_e)$ introduced in Assumption 1. It is easy to verify that there exists a strictly positive number ϵ such that $(\bar{\mathbf{p}}_n, \bar{\mathbf{p}}_e)$ is feasible for the CGNF with strict inequality in (6c), where $\bar{p}_{ij} = p_{ij}$ and $\bar{p}_{ji} = p_{ji} + \epsilon$ for every $(i,j) \in \overrightarrow{\mathcal{E}}$ and $\bar{\mathbf{p}}_n$ is associated with $\bar{\mathbf{p}}_e$. ■

Let $\lambda_i^{\min}$ and $\lambda_i^{\max}$ denote optimal Lagrange multipliers corresponding to the constraints $p_i^{\min} \leq p_i$ and $p_i \leq p_i^{\max}$. Assume that $(\bar{\mathbf{p}}_n^*, \bar{\mathbf{p}}_e^*)$ is an optimal solution of the GNF problem. Using the duality theorem, it can be shown that changing the objective function to

$$\sum_{i\in\mathcal{N}} f_i(p_i) - \lambda_i^{\min}(p_i - p_i^{\min}) + \lambda_i^{\max}(p_i - p_i^{\max}) \tag{55}$$

would not affect the optimal solution [15]. Furthermore, it follows from the first-order optimality conditions that

$$(\bar{\mathbf{p}}_n^*, \bar{\mathbf{p}}_e^*) = \underset{\mathbf{p}_n \in \mathbb{R}^m, \mathbf{p}_e \in \mathcal{B}_e}{\arg\min} \quad \sum_{i \in \mathcal{N}} \lambda_i p_i \tag{56a}$$

$$\text{subject to} \quad p_i = \sum_{j \in \mathcal{N}(i)} p_{ij}, \qquad \forall i \in \mathcal{N} \tag{56b}$$

$$f_{ij}(p_{ij}) \leq p_{ji}, \qquad \forall (i,j) \in \overrightarrow{\mathcal{E}} \tag{56c}$$

$$p_{ij} \in [p_{ij}^{\min}, p_{ij}^{\max}], \quad \forall (i,j) \in \mathcal{E} \tag{56d}$$

where

$$\lambda_i = f_i'(\bar{p}_i^*) - \lambda_i^{\min} + \lambda_i^{\max}, \qquad \forall i \in \mathcal{N} \tag{57}$$

Hence,

$$(\bar{p}_{ij}^*, \bar{p}_{ji}^*) = \underset{(p_{ij}, p_{ji}) \in \mathbb{R}^2}{\arg\min} \quad \lambda_i p_{ij} + \lambda_j p_{ji} \tag{58a}$$

$$\text{subject to} \quad f_{ij}(p_{ij}) \leq p_{ji}, \tag{58b}$$

$$p_{ij} \in [p_{ij}^{\min}, p_{ij}^{\max}], \tag{58c}$$

$$p_{ji} \in [p_{ji}^{\min}, p_{ji}^{\max}] \tag{58d}$$

for every $(i,j) \in \overrightarrow{\mathcal{E}}$.

Definition 9 *Define $\mathcal{V}$ as the set of all indices $i \in \mathcal{N}$ for which $\lambda_i \leq 0$. Define $\bar{\mathcal{V}}$ as the set of all indices $i \in \mathcal{N} \backslash \mathcal{V}$ for which there exists a vertex $j \in \mathcal{V}$ such that $(i,j) \in \mathcal{G}$ (i.e., $\bar{\mathcal{V}}$ denotes the set of the neighbors of $\mathcal{V}$ in the graph $\mathcal{G}$).*

Since the objective function of the optimization problem (58) is linear, it is straightforward to verify that $f_{ij}(\bar{p}_{ij}^*) = \bar{p}_{ji}^*$ as long as $\lambda_i > 0$ or $\lambda_j > 0$. In particular,

$$f_{ij}(\bar{p}_{ij}^*) = \bar{p}_{ji}^*, \qquad \forall (i,j) \in \overrightarrow{\mathcal{E}}, \ \{i,j\} \not\subseteq \mathcal{V} \tag{59a}$$

$$\bar{p}_{ij}^* = p_{ij}^{\min}, \qquad \forall (i,j) \in \mathcal{E}, \ i \in \bar{\mathcal{V}}, \ j \in \mathcal{V} \tag{59b}$$

If $f_{ij}(\bar{p}_{ij}^*)$ were equal to $\bar{p}_{ji}^*$ for every $(i,j) \in \overrightarrow{\mathcal{E}}$, then the proof of Part 1 of Theorem 2 was complete. However, the relation $f_{ij}(\bar{p}_{ij}^*) < \bar{p}_{ji}^*$ might hold in theory if $(i,j) \in \overrightarrow{\mathcal{E}}$ and $\{i,j\} \subseteq \mathcal{V}$. Hence, is important to study this scenario.

Proof of Part 1 of Theorem 2 in the general case: For every given index $i \in \mathcal{V}$, the term λ_i is nonpositive by definition. On the other hand, $f_i'(\cdot)$ is strictly positive (since $f_i(\cdot)$ is monotonically increasing), and $\lambda_i^{\min}$ and $\lambda_i^{\max}$ are both nonnegative (since they are the Lagrange multipliers for inequality constraints). Therefore, it follows from (57) that $\lambda_i^{\min} > 0$, implying that

$$\bar{p}_i^* = p_i^{\min}, \qquad \forall i \in \mathcal{V} \tag{60}$$

Thus,

$$p_i^* \geq p_i^{\min} = \bar{p}_i^*, \qquad \forall i \in \mathcal{V} \tag{61}$$

Let $\mathcal{G}_s$ denote a subgraph of $\mathcal{G}$ with the vertex set $\mathcal{V} \cup \bar{\mathcal{V}}$ that includes those edges $(i,j) \in \mathcal{E}$ satisfying either of the following conditions:

- $\{i,j\} \subseteq \mathcal{V}$
- $i \in \mathcal{V}$ and $j \in \bar{\mathcal{V}}$.

Note that $\mathcal{G}_s$ includes all edges of $\mathcal{G}$ within the vertex subset $\mathcal{V}$ and those between the sets $\mathcal{V}$ and $\bar{\mathcal{V}}$, but this subgraph contains no edge between the vertices in $\bar{\mathcal{V}}$. The first objective is to show that

$$p_i^*(\mathcal{G}_s) \geq \bar{p}_i^*(\mathcal{G}_s), \qquad \forall i \in \mathcal{V} \cup \bar{\mathcal{V}} \tag{62}$$

To this end, two possibilities will be investigated:

- *Case 1)* Consider a vertex $i \in \mathcal{V}$. Given each edge $(i,j) \in \mathcal{E}$, vertex j must belong to $\mathcal{V} \cup \bar{\mathcal{V}}$, due to Definition 9. Hence, $p_i^*(\mathcal{G}_s) = p_i^*$ and $\bar{p}_i^*(\mathcal{G}_s) = \bar{p}_i^*$. Combining these equalities with (61) gives rise to $p_i^*(\mathcal{G}_s) \geq \bar{p}_i^*(\mathcal{G}_s)$.
- *Case 2)* Consider a vertex $i \in \bar{\mathcal{V}}$. Based on (59b), One can write:

$$\bar{p}_i^*(\mathcal{G}_s) = \sum_{j \in \mathcal{V} \cap \mathcal{N}(i)} \bar{p}_{ij}^* = \sum_{j \in \mathcal{V} \cap \mathcal{N}(i)} p_{ij}^{\min} \tag{63}$$

  Similarly,

$$p_i^*(\mathcal{G}_s) = \sum_{j \in \mathcal{V} \cap \mathcal{N}(i)} p_{ij}^* \geq \sum_{j \in \mathcal{V} \cap \mathcal{N}(i)} p_{ij}^{\min} \tag{64}$$

  Thus, $p_i^*(\mathcal{G}_s) \geq \bar{p}_i^*(\mathcal{G}_s)$.

So far, inequality (62) has been proven. Consider $\tilde{\mathbf{p}}_n$ introduced in (53). Similar to (54), it is straightforward to show that $\tilde{p}_i(\mathcal{G}_s) \leq \bar{p}_i^*(\mathcal{G}_s)$ for every $i \in \mathcal{V} \cup \bar{\mathcal{V}}$. Hence,

$$\tilde{\mathbf{p}}_n(\mathcal{G}_s) \leq \bar{\mathbf{p}}_n^*(\mathcal{G}_s) \leq \mathbf{p}_n^*(\mathcal{G}_s) \tag{65}$$

On the other hand, $\tilde{\mathbf{p}}_n(\mathcal{G}_s)$ and $\mathbf{p}_n^*(\mathcal{G}_s)$ are both in $\mathcal{P}(\mathcal{G}_s)$. Using (65) and Theorem 1 (but for $\mathcal{G}_s$ as opposed to $\mathcal{G}$), it can be concluded that $\bar{\mathbf{p}}_n^*(\mathcal{G}_s) \in \mathcal{P}(\mathcal{G}_s)$. Hence, there exists a flow vector $\hat{\mathbf{p}}_e(\mathcal{G}_s)$ associated with $\bar{\mathbf{p}}_n^*(\mathcal{G}_s)$, meaning that

$$\bar{p}_i^*(\mathcal{G}_s) = \sum_{j \in \mathcal{N}(i) \cap (\mathcal{V} \cup \bar{\mathcal{V}})} \hat{p}_{ij}(\mathcal{G}_s), \qquad \forall i \in \mathcal{V} \tag{66a}$$

$$\bar{p}_i^*(\mathcal{G}_s) = \sum_{j \in \mathcal{N}(i) \cap \mathcal{V}} \hat{p}_{ij}(\mathcal{G}_s), \qquad \forall i \in \bar{\mathcal{V}} \tag{66b}$$

$$\hat{p}_{ji}(\mathcal{G}_s) = f_{ij}(\hat{p}_{ij}(\mathcal{G}_s)), \qquad \forall (i,j) \in \overrightarrow{\mathcal{G}}_s \tag{66c}$$

Now, one can expand $\hat{\mathbf{p}}_e(\mathcal{G}_s)$ to $\hat{\mathbf{p}}_e$ as

$$\hat{p}_{jk} = \begin{cases} \hat{p}_{jk}(\mathcal{G}_s) & \text{if} \quad (j,k) \in \mathcal{G}_s \\ \bar{p}_{jk}^* & \text{otherwise} \end{cases}, \quad \forall (j,k) \in \mathcal{E} \tag{67}$$

Let $\hat{\mathbf{p}}_n$ denote the injection vector associated with the flow vector $\hat{\mathbf{p}}_e$. Two observations can be made:

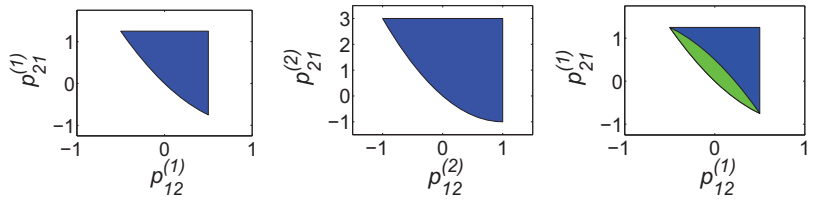

(a) (b) (c)

Fig. 7: Figures (a) and (b) show the feasible sets $\mathcal{T}_{\rm c}^{(1)}$ and $\mathcal{T}_{\rm c}^{(2)}$ for Example 3, respectively. Figure (c) is aimed to show that CGNF may have an infinite number of solutions (all points in the yellow area may be the solutions of GNF).

1) $\hat{\mathbf{p}}_n$ is equal to $\bar{\mathbf{p}}_n^*$.
2) Due to (59a), (66c) and (67), $(\hat{\mathbf{p}}_n, \hat{\mathbf{p}}_e)$ is a feasible point of GNF.

This means that $\bar{\mathbf{p}}_n^*$ is the unique optimal solution of Geometric CGNF and yet a feasible point of Geometric GNF. The rest of the proof is the same as the proof of Theorem 2 under Condition (50) (given earlier). ■

Next example is provided to understand the reason why CGNF may fail to obtain a correct flow vector associated with the optimal injection vector.

Example 3: Consider again the illustrative example studied in Section 3.1, corresponding to the graph $\mathcal{G}$ depicted in Figure 1. Let $\mathcal{T}$ denote the projection of the feasible set of the GNF problem given in (8) over the flow space associated with the vector $(p_{12}^{(1)}, p_{21}^{(1)}, p_{12}^{(2)}, p_{21}^{(2)})$. It is easy to verify that $\mathcal{T}$ can be decomposed as the product of $\mathcal{T}^{(1)}$ and $\mathcal{T}^{(2)}$, where

$$\mathcal{T}^{(1)} = \left\{ (p_{12}^{(1)}, p_{21}^{(1)}) \;\middle|\; p_{12}^{(1)} \in [-0.5, 0.5],\ p_{21}^{(1)} = \left(p_{12}^{(1)} - 1\right)^2 - 1 \right\}$$

and

$$\mathcal{T}^{(2)} = \left\{ (p_{12}^{(2)}, p_{21}^{(2)}) \;\middle|\; p_{12}^{(2)} \in [-1, 1],\ p_{21}^{(2)} = \left(p_{12}^{(2)} - 1\right)^2 - 1 \right\}$$

Likewise, define $\mathcal{T}_{\rm c}$ as the projection of the feasible set of the CGNF problem over its flow space. As before, $\mathcal{T}_{\rm c}$ can be written as $\mathcal{T}_{\rm c}^{(1)} \times \mathcal{T}_{\rm c}^{(2)}$, where $\mathcal{T}_{\rm c}^{(i)}$ is obtained from $\mathcal{T}^{(i)}$ by changing its equality

$$p_{21}^{(i)} = \left(p_{12}^{(i)} - 1\right)^2 - 1 \tag{68}$$

to the inequality

$$p_{21}^{(i)} \geq \left(p_{12}^{(i)} - 1\right)^2 - 1 \tag{69}$$

for $i = 1, 2$, and adding the limits $p_{21}^{(1)} \leq 1.5^2 - 1$ and $p_{21}^{(2)} \leq 2^2 - 1$. The sets $\mathcal{T}_{\rm c}^{(1)}$ and $\mathcal{T}_{\rm c}^{(2)}$ are drawn in Figures 7(a) and 7(b). Given $i \in \{1, 2\}$, note that

$\mathcal{T}_c^{(i)}$ has two flat boundaries and one curvy (lower) boundary that is the same as $\mathcal{T}^{(i)}$. Consider the flow vector $(\bar{p}_{12}^{(1)}, \bar{p}_{21}^{(1)}, \bar{p}_{12}^{(2)}, \bar{p}_{21}^{(2)}) \in \mathcal{T}_c$ defined as

$$\begin{aligned} \left(\bar{p}_{12}^{(1)}, \bar{p}_{21}^{(1)}\right) &= \left(0.5, (0.5-1)^2 - 1\right), \\ \left(\bar{p}_{12}^{(2)}, \bar{p}_{21}^{(2)}\right) &= \left(-0.5, (-0.5-1)^2 - 1\right) \end{aligned} \tag{70}$$

Define $\bar{p}_1 = \bar{p}_{12}^{(1)} + \bar{p}_{12}^{(2)}$ and $\bar{p}_2 = \bar{p}_{21}^{(1)} + \bar{p}_{21}^{(2)}$. It can be verified that for every point $(\tilde{p}_{12}^{(1)}, \tilde{p}_{21}^{(1)})$ in the green area of Figure 7(c), there exists a vector $(\tilde{p}_{12}^{(2)}, \tilde{p}_{21}^{(2)}) \in \mathcal{T}_c^{(2)}$ such that

$$\bar{p}_1 = \tilde{p}_{12}^{(1)} + \tilde{p}_{12}^{(2)}, \quad \bar{p}_2 = \tilde{p}_{21}^{(1)} + \tilde{p}_{21}^{(2)} \tag{71}$$

This means that if $(\bar{p}_1, \bar{p}_2, \bar{p}_{12}^{(1)}, \bar{p}_{21}^{(1)}, \bar{p}_{12}^{(2)}, \bar{p}_{21}^{(2)})$ turns out to be an optimal solution of CGNF, then $(\bar{p}_1, \bar{p}_2, \tilde{p}_{12}^{(1)}, \tilde{p}_{21}^{(1)}, \tilde{p}_{12}^{(2)}, \tilde{p}_{21}^{(2)})$ becomes another solution of CGNF. As a result, although Geometric CGNF has a unique solution (optimal injection vector), CGNF may have an infinite number of solutions whose corresponding flow vectors do not necessarily satisfy the constraints of GNF. ■

So far, we have shown that CGNF always finds the optimal injection vector and optimal objective value for the GNF problem. In addition, it finds the optimal flow vector if the injection vector is a Pareto point. Now, we consider the case where the optimal injection vector is not necessarily Pareto but lies on the boundary of the injection region. The objective is to prove that the network $\mathcal{G}$ can be decomposed into two subgraphs $\mathcal{G}_1$ and $\mathcal{G}_2$ such that: (i) the flows obtained from CGNF are optimal (feasible) for GNF for those lines inside $\mathcal{G}_1$ or between $\mathcal{G}_1$ and $\mathcal{G}_2$, (ii) the flows over the lines between $\mathcal{G}_1$ and $\mathcal{G}_2$ all hit their limits at optimality.

Definition 10 *Define $\mathcal{G}_1$ and $\mathcal{G}_2$ as the subgraphs of $\mathcal{G}$ induced by the vertex subsets $\mathcal{N}\backslash\mathcal{V}$ and $\mathcal{V}$, respectively.*

Theorem 3 *Assume that $f_i(\cdot)$ is strictly convex for every $i \in \mathcal{N}$. Let $(\mathbf{p}_n^*, \mathbf{p}_d^*)$ and $(\mathbf{p}_n^*, \bar{\mathbf{p}}_d^*)$ denote arbitrary globally optimal solutions of the GNF and CGNF problems, respectively. The following relations hold:*

$$p_{ij}^* = \bar{p}_{ij}^*, \qquad \forall (i,j) \in \mathcal{N}\backslash\mathcal{V} \tag{72a}$$

$$p_{ji}^* = \bar{p}_{ji}^* = p_{ji}^{\max}, \qquad \forall (i,j) \in (\mathcal{N}\backslash\mathcal{V} \times \mathcal{V}) \cap \mathcal{E} \tag{72b}$$

Proof: Since every solution of GNF is a solution of CGNF as well (due to Theorem 2), the points $(\mathbf{p}_n^*, \mathbf{p}_d^*)$ and $(\mathbf{p}_n^*, \bar{\mathbf{p}}_d^*)$ are both solutions of CGNF. Now, it follows from the duality theorem that $(\mathbf{p}_n^*, \mathbf{p}_d^*)$ and $(\mathbf{p}_n^*, \bar{\mathbf{p}}_d^*)$ are both minimizers of (56) and (58). Since the objective of (58) is linear and $f_i(\cdot)$ is strictly convex, it can be concluded that:

- The optimization problem (58) has a unique solution as long as $\lambda_i^* > 0$ or $\lambda_j^* > 0$.
- (p_{ij}, p_{ji}) becomes equal to $(p_{ij}^{\min}, p_{ji}^{\max})$ at optimality if $\lambda_i^* > 0$ and $\lambda_j^* \leq 0$.

– (p_{ij}, p_{ji}) becomes equal to $(p_{ij}^{\max}, p_{ji}^{\min})$ at optimality if $\lambda_j^* > 0$ and $\lambda_i^* \leq 0$.

Equations (72a) and (72b) follow immediately from the above properties. ■

Corollary 2 *Let $(\mathbf{p}_n^*, \mathbf{p}_d^*)$ and $(\mathbf{p}_n^*, \bar{\mathbf{p}}_d^*)$ denote arbitrary globally optimal solutions of the GNF and CGNF problems, respectively. If there exists a vertex $i \in \mathcal{N}$ such that $\bar{p}_i^* > p_i^{\min}$, then $\mathbf{p}_d^*$ and $\bar{\mathbf{p}}_d^*$ must be identical in at least one entry.*

Proof: Consider a vertex $i \in \mathcal{N}$ such that $\bar{p}_i^* > p_i^{\min}$. It follows from (57) that λ_i^* is positive. Now, Definition 10 yields that the subgraph $\mathcal{G}_1$ is nonempty. The proof is an immediate consequence of Theorem 3. ■

Definition 11 *Consider a solution $(\mathbf{p}_n^*, \mathbf{p}_d^*)$ of GNF. A line $(i, j) \in \mathcal{E}$ of the network $\mathcal{G}$ is called "congested" if p_{ij}^* is equal to $p_{ij}^{\max}$ or p_{ji}^* is equal to $p_{ji}^{\max}$.*

Corollary 3 *Let $(\mathbf{p}_n^*, \mathbf{p}_d^*)$ and $(\mathbf{p}_n^*, \bar{\mathbf{p}}_d^*)$ denote arbitrary globally optimal solutions of the GNF and CGNF problems, respectively. Assume that there exists a vertex $i \in \mathcal{N}$ such that $\bar{p}_i^* > p_i^{\min}$. If the network $\mathcal{G}$ has no congested line, then GNF and CGNF are equivalent, i.e., $(\mathbf{p}_n^*, \mathbf{p}_d^*) = (\mathbf{p}_n^*, \bar{\mathbf{p}}_d^*)$.*

Proof: Due to the proof of Corollary 2, the set $\mathcal{N} \backslash \mathcal{V}$ is nonempty. On the other hand, since the network $\mathcal{G}$ has no congested line by assumption, it can be concluded from Theorem 3 that $(\mathcal{N} \backslash \mathcal{V} \times \mathcal{V}) \cap \mathcal{E}$ is an empty set. Therefore, $\mathcal{V}$ must be empty, which implies the equivalence of GNF and CGNF due to Theorem 3. ■

3.4 Characterization of Optimal Flow Vectors

In this section, we aim to characterize the set of all optimal flow vectors for GNF, based on the optimal injection vector found using CGNF. In particular, we will show that this set could be nonconvex and disconnected. Before presenting the results, it is helpful to illustrate the key ideas in an example.

Example 4: Consider the graph $\mathcal{G}$ depicted in Figure 8(a), which consists of two cycles and four nodes. Let $(\mathbf{p}_n^*, \mathbf{p}_e^*)$ denote an arbitrary solution of GNF, where $\mathbf{p}_n^*$ is obtained from CGNF and $\mathbf{p}_e^*$ is to be found. The objective of this example is to demonstrate that all optimal flows in the network can be uniquely characterized in terms of two flows. Consider the unknown flows p_{12}^* and p_{13}^*. One can write

$$p_{24}^* = p_2^* - f_{12}(p_{12}^*) \tag{73a}$$
$$p_{34}^* = p_3^* - f_{13}(p_{13}^*) \tag{73b}$$
$$p_{14}^* = p_1^* - p_{12}^* - p_{13}^* \tag{73c}$$

It follows from the above equations that all flows in the network can be cast as functions of (p_{12}^*, p_{13}^*), and in addition $(p_{12}, p_{13}) = (p_{12}^*, p_{13}^*)$ is a solution

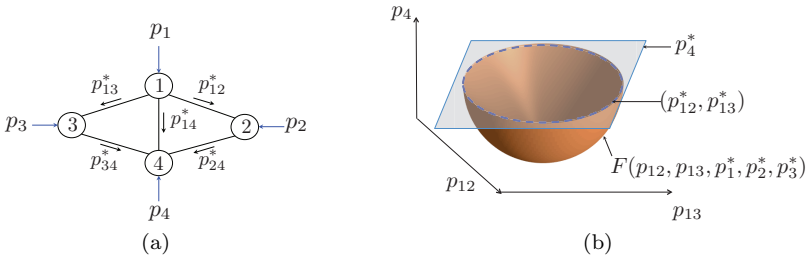

Fig. 8: (a) The 2-cycle graph studied in Example 5; (b): visualization of the level-set problem used to find optimal flows for Example 5.

to the level-set problem $F(p_{12}, p_{13}, p^*_1, p^*_2, p^*_3) = p^*_4$, where

$$\begin{aligned} F(p_{12}, p_{13}, p_1, p_2, p_3) = {} & f_{24}\left(p_2 - f_{12}(p_{12})\right) \\ & + f_{34}\left(p_3 - f_{13}(p_{13})\right) \\ & + f_{14}\left(p_1 - p_{12} - p_{13}\right) \end{aligned} \tag{74}$$

is a convex function with respect to (p_{12}, p_{13}) but not necessarily monotonic. On the other hand, the equations in (73) can be used to translate the box constraints on all flows to certain constraints only on p^*_{12} and p^*_{13}:

$$\tilde{p}^{\min}_{12} \le p^*_{12} \le \tilde{p}^{\max}_{12} \tag{75a}$$
$$\tilde{p}^{\min}_{13} \le p^*_{13} \le \tilde{p}^{\max}_{13} \tag{75b}$$
$$p^{\min}_{14} \le p^*_1 - p^*_{12} - p^*_{13} \le p^{\max}_{14} \tag{75c}$$

for some numbers $\tilde{p}^{\min}_{12}, \tilde{p}^{\max}_{12}, \tilde{p}^{\min}_{13}, \tilde{p}^{\max}_{13}$. Let C_1 and C_2 denote the sets of all points (p^*_{12}, p^*_{13}) satisfying the level-set problem $F(p^*_{12}, p^*_{13}, p^*_1, p^*_2, p^*_3) = p^*_4$ and the reformulated flow constraints (75), respectively. The set of all optimal flow solutions (p^*_{12}, p^*_{13}) can be expressed as $\mathcal{C}_1 \cap \mathcal{C}_2$, where $\mathcal{C}_1$ is the boundary of a convex set (corresponding to $F(\cdot)$) and $\mathcal{C}_2$ is a polytope. As illustrated in Figure 8(b), $\mathcal{C}_1$ is the boundary of a convex set, and therefore its intersection with a polytope (e.g., a box) could form up to 4 disconnected components. In summary, the optimal flow vectors for GNF may constitute a nonconvex infinite set, consisting of as high as 4 disconnected components. ■

By following the argument used in Example 5, it is straightforward to show that if the graph $\mathcal{G}$ is a tree, the optimal flow vector is unique and can be easily obtained from the optimal injection vector $\mathbf{p}^*_n$. Hence, the main challenge is to deal with mesh flow networks. To this end, consider an arbitrary spanning tree of the m-node graph $\mathcal{G}$, denoted as $\mathcal{G}_t$. Let $\mathbf{p}_{dt}$ denote a sub-vector of the semi-flow vector $\mathbf{p}_d$ associated with those edges of $\mathcal{G}$ that do not exist in $\mathcal{G}_t$. Recall that $\overrightarrow{\mathcal{G}}$ was obtained through an arbitrary orientation of the edges of the graph $\mathcal{G}$. With no loss of generality, one can consider $\mathcal{G}_t$ as a rooted tree with node m as its root, where all arcs of $\overrightarrow{\mathcal{G}}$ are directed toward the root.

Lemma 6 *There exist convex functions $F_{ij} : \mathbb{R}^{|\mathcal{E}|} \to \mathbb{R}$ for all $(i,j) \in \overrightarrow{\mathcal{E}}$ such that the following statements hold:*

1) Given every arbitrary feasible solution $(\mathbf{p}_n, \mathbf{p}_e)$ of the GNF problem, the relations

$$p_{ji} = F_{ij}(\mathbf{p}_{dt}, p_1, p_2, ..., p_{m-1}), \qquad \forall (i,j) \in \overrightarrow{\mathcal{E}} \tag{76}$$

are satisfied.

2) The function $F(\mathbf{p}_{dt}, p_1, p_2, ..., p_{m-1})$ defined as

$$\sum_{j \in \mathcal{N}(m)} F_{jm}(\mathbf{p}_{dt}, p_1, p_2, ..., p_{m-1}) \tag{77}$$

is convex.

Proof: The proof is in line with the technique used in Example 4. The details are omitted for brevity. ■

Definition 12 *Define $\mathcal{C}_1$ as the set of all vectors $\mathbf{p}_{dt}$ satisfying the level-set problem $F(\mathbf{p}_{dt}, p_1^*, p_2^*, ..., p_{m-1}^*) = p_m^*$. Also, define $\mathcal{C}_2$ as the set of all vectors $\mathbf{p}_{dt}$ satisfying the inequalities*

$$p_{ji}^{\min} \leq F_{ij}(\mathbf{p}_{dt}, p_1^*, p_2^*, ..., p_{m-1}^*) \leq p_{ji}^{\max}, \qquad \forall (i,j) \in \overrightarrow{\mathcal{E}} \tag{78}$$

Theorem 4 *A flow vector $\mathbf{p}_e^*$ is globally optimal for GNF if and only if*

$$\mathbf{p}_{dt}^* \in \mathcal{C}_1 \cap \mathcal{C}_2 \tag{79a}$$

$$p_{ji}^* = F_{ij}(\mathbf{p}_{dt}^*, p_1^*, p_2^*, ..., p_{m-1}^*), \qquad \forall (i,j) \in \overrightarrow{\mathcal{E}} \tag{79b}$$

$$p_{ij}^* = f_{ji}(p_{ji}^*), \qquad \forall (i,j) \in \overrightarrow{\mathcal{E}} \tag{79c}$$

Proof: The proof is based on Lemma 6 and the technique used in Example 4. The details are omitted for brevity. ■

Theorem 4 states that: (i) the set of optimal flow vectors can be characterized in terms of the unique optimal injection vector as well as the flow sub-vector $\mathbf{p}_{dt}$, (ii) the set of optimal flow sub-vectors $\mathbf{p}_{dt}^*$ is the collection of all points in the intersection of $\mathcal{C}_1$ and $\mathcal{C}_2$. Moreover, in light of Lemma 6, $\mathcal{C}_1$ is the boundary of a convex set. Although $\mathcal{C}_2$ was shown to be a polytope in Examples 4 and 5, it is non-convex in general. Since $\mathcal{C}_1$ is the boundary of a convex set, it occurs that the intersection of $\mathcal{C}_2$ with $\mathcal{C}_1$ may lead to as high as $2^{|\mathcal{E}|-|\mathcal{N}|+1}$ disconnected components, all lying on the boundary of a convex set (note that $|\mathcal{E}| - |\mathcal{N}| + 1$ is the size of the vector $\mathbf{p}_{dt}$).

3.5 Extended GNF Problem

In this subsection, we generalize the results developed for the GNF problem to the case where there are global convex constraints coupling the flows and/or injections of different parts of the network, in addition to the local constraints over individual lines and at separate nodes.

Definition 13 *Consider a set of convex constraints* $g_i(\mathbf{p}_n, \mathbf{p}_e) \leq 0$ *for* $i = 1, 2, ..., k$, *which are called* coupling constraints. *The* extended GNF problem *is defined as* (4) *subject to this set of coupling constraints. Denote* $\mathcal{P}^e$ *as the set of all vectors* $\mathbf{p}_n$ *for which there exists a vector* $\mathbf{p}_e$ *such that* $(\mathbf{p}_n, \mathbf{p}_e)$ *is feasible for the extended GNF problem. The above set of coupling constraints is referred to as* box-preserving *if its addition to the GNF problem preserves the box property of the injection region, meaning that the box* $\mathcal{B}(\mathbf{p}_n, \tilde{\mathbf{p}}_n)$ *is contained in* $\mathcal{P}^e$ *for every two points* $\mathbf{p}_n$ *and* $\tilde{\mathbf{p}}_n$ *in* $\mathcal{P}^e$.

Theorem 5 *Consider the extended GNF problem with the coupling constraints* $g_i(\mathbf{p}_n, \mathbf{p}_e) \leq 0$ *for every* $i \in \{1, 2, ..., k\}$. *This set of constraints is guaranteed to be box-preserving if either of the following conditions is satisfied:*

1) $\mathcal{G}$ *is a tree and the function* $g_i(\mathbf{p}_n, \mathbf{p}_e)$ *is non-decreasing with respect to all entries of* $\mathbf{p}_n$ *and* $\mathbf{p}_e$, *for every* $i \in \{1, 2, ..., k\}$.
2) The function $g_i(\mathbf{p}_n, \mathbf{p}_e)$ *does not depend on* $\mathbf{p}_e$ *and is non-decreasing with respect to all entries of* $\mathbf{p}_n$, *for every* $i \in \{1, 2, ..., k\}$.

Proof: The box-preserving property under Condition 2 follows from the fact that whenever the coupling constraints are non-decreasing functions of the injection vector, if $\mathbf{p}_n$ satisfies the constraints, any other injection vector $\tilde{\mathbf{p}}_n$ with the property $\tilde{\mathbf{p}}_n \leq \mathbf{p}_n$ also satisfies the constraints.

To prove the box-preserving property under Condition 1, it suffices to show that if $\mathcal{G}$ is a tree, every flow p_{ij} can be written as a non-decreasing function of $\mathbf{p}_n$ (then the proof follows from Condition 2 of the theorem). Consider $\mathcal{G}$ as a rooted tree with an arbitrary node at the root. Recall that $\overrightarrow{\mathcal{G}}$ was obtained through an arbitrary orientation of the edges of $\mathcal{G}$. Without loss of generality, assume that the directions of all edges are toward the root. Define h as the depth of $\mathcal{G}$ (maximum distance of every leaf from the root). Assume that a node with the distance t from the root is identified by i_t. First, we use induction to show that the flows going toward the root can be written as non-decreasing functions of the injection vector. We start with the farthest nodes from the root. For each node i_h, one can write $p_{i_h i_{h-1}} = p_{i_h}$, which is non-decreasing in terms of the injection vector. Now, for every flow $p_{i_t i_{t-1}}$ with $0 \leq t \leq h-1$, one can write

$$p_{i_t i_{t-1}} = p_{i_t} - \sum_{(j_{t+1}, i_t) \in \mathcal{E}} f_{j_{t+1}, i_t}(p_{j_{t+1} i_t}) \tag{80}$$

By the induction hypothesis, $p_{j_{t+1} i_t}$ can be written as a non-decreasing function of the injection vector. Therefore, (80) implies that the same statement holds for $p_{i_t i_{t-1}}$.

Now, we use another inductive argument to show that each flow going toward the leaves can be written as a non-decreasing function of the injection vector. We start from the root node. For every flow $p_{i_0 i_1}$, one can write

$$p_{i_0 i_1} = p_{i_0} - \sum_{\substack{(j_1,i_0)\in\mathcal{E} \\ j_1 \neq i_1}} f_{j_1,i_0}(p_{j_1 i_0}) \tag{81}$$

which implies that $p_{i_0 i_1}$ is a non-decreasing function of the injection vector (note that this property holds for $p_{j_1 i_0}$). For every flow $p_{i_{t-1} i_t}$ with $2 \leq t \leq h$, one can verify that

$$p_{i_{t-1} i_t} = p_{i_{t-1}} - f^{-1}_{i_{t-1} i_{t-2}}(p_{i_{t-2} i_{t-1}}) - \sum_{\substack{(j_1,i_0)\in\mathcal{E} \\ j_t \neq i_t}} f_{j_t,i_{t-1}}(p_{j_t i_{t-1}}) \tag{82}$$

The proof is completed by observing that

- $f^{-1}_{i_{t-1} i_{t-2}}(\cdot)$ is a decreasing function.
- $p_{i_{t-2} i_{t-1}}$ is a non-decreasing function of the injection vector due to the induction hypothesis.
- $p_{j_t i_{t-1}}$ is a non-decreasing function of the injection vector since its direction is toward the root. ■

In the rest of this subsection, we assume that the set of coupling constraints in the extended GNF problem is box-preserving.

Corollary 4 *Consider two arbitrary points $\hat{\mathbf{p}}_n$ and $\tilde{\mathbf{p}}_n$ belonging to the box-constrained injection region $\mathcal{P}^e \cap \mathcal{B}$. The box $\mathcal{B}(\hat{\mathbf{p}}_n, \tilde{\mathbf{p}}_n)$ is contained in $\mathcal{P}^e \cap \mathcal{B}$.*

Proof: The proof follows immediately from the definition of $\mathcal{P}^e$ and Definition 13. ■

Define the extended CGNF problem as CGNF subject to the additional constraints $g_i(\mathbf{p}_n, \mathbf{p}_e) \leq 0$ for $i = 1, 2, ..., k$. Note that this problem is convex.

Theorem 6 *Assume that the extended GNF problem is feasible. Let $(\mathbf{p}^*_n, \mathbf{p}^*_e)$ and $(\bar{\mathbf{p}}^*_n, \bar{\mathbf{p}}^*_e)$ denote arbitrary globally optimal solutions of the extended GNF and extended CGNF problems, respectively. The following relations hold:*

1) $\mathbf{p}^*_n = \bar{\mathbf{p}}^*_n$
2) $(\bar{\mathbf{p}}^*_n, \bar{\mathbf{p}}^*_e)$ *is a solution of the extended GNF problem, provided that $\mathbf{p}^*_n$ is a Pareto point in $\mathcal{P}^e$.* ■

Proof: The argument made in the proof of Theorem 2 can be adopted to prove this theorem. The details are omitted for brevity. ■

3.6 Optimal Power Flow in Electrical Power Networks

In this subsection, the results derived earlier for the GNF and extended GNF problems will be applied to power networks. Consider a group of generators

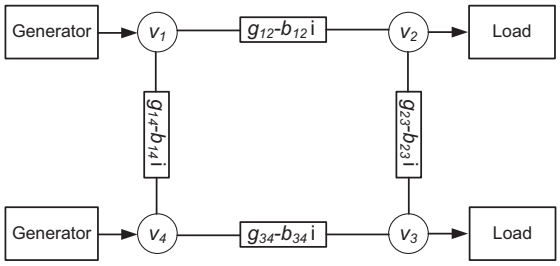

Fig. 9: An example of electrical power network.

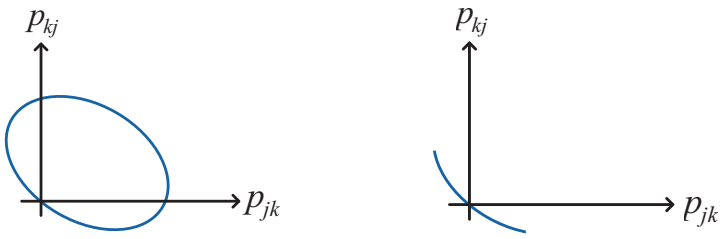

(a) (b)

Fig. 10: (a) Feasible set for (p_{jk}, p_{kj}); (b) feasible set for (p_{jk}, p_{kj}) after imposing lower and upper bounds on θ_{jk}.

(sources of energy), which are connected to a group of electrical loads (consumers) via an electrical power network (grid). This network comprises a set of lines connecting various nodes to each other (e.g., a generator to a load). Figure 9 exemplifies a four-node power network with two generators and two loads. Each load requests certain amount of energy, and the question of interest is to find the most economical power dispatch by the generators such that the demand and network constraints are satisfied. To formulate the problem, let $\mathcal{G}$ denote the flow network corresponding to the electrical power network, where

- The injection p_j at node $j \in \mathcal{N}$ represents either the active power produced by a generator and injected to the network or the active power absorbed from the network by an electrical load.
- The flow p_{jk} over each line $(j,k) \in \mathcal{E}$ represents the active power entering the line (j,k) from its j endpoint.

The problem of optimizing the flows in a power network is called "optimal power flow (OPF)".

Let v_i denote the complex (phasor) voltage at node $i \in \mathcal{N}$ of the power network. Denote the phase of v_i as θ_i. Given an edge $(j,k) \in \mathcal{G}$, we denote the admittance of the line between nodes j and k as $g_{jk} - \mathrm{i}b_{jk}$, where the symbol

i denotes the imaginary unit. g_{jk} and b_{jk} are nonnegative numbers due to the passivity of the line. There are two active flows entering the line (j,k) from its both ends. These flows are given by the equations:

$$p_{jk} = |v_j|^2 g_{jk} + |v_j||v_k|b_{jk}\sin(\theta_{jk}) - |v_j||v_k|g_{jk}\cos(\theta_{jk}),$$
$$p_{kj} = |v_k|^2 g_{jk} - |v_j||v_k|b_{jk}\sin(\theta_{jk}) - |v_j||v_k|g_{jk}\cos(\theta_{jk})$$

where $\theta_{jk} = \theta_j - \theta_k$. First, consider the distribution system where the underlying network is a tree. For now, assume that $|v_j|$ and $|v_k|$ are fixed at their nominal values, while θ_{jk} is a variable to be designed. If θ_{jk} varies from $-\pi$ to π, then the feasible set of (p_{jk}, p_{kj}) becomes an ellipse, as illustrated in Figure 10(a). It can be observed that p_{kj} cannot be written as a function of p_{jk}. This observation is based on the implicit assumption that there is no limit on θ_{jk}. Suppose that θ_{jk} must belong to an interval $[-\theta_{jk}^{\max}, \theta_{jk}^{\max}]$ for some angle $\theta_{jk}^{\max}$. If the new feasible set for (p_{jk}, p_{kj}) resembles the partial ellipse drawn in Figure 10(b), then p_{kj} can be expressed as $f_{jk}(p_{jk})$ for a monotonically decreasing and convex function $f_{jk}(\cdot)$. This occurs if

$$\theta_{jk}^{\max} \leq \tan^{-1}\left(\frac{b_{jk}}{g_{jk}}\right) \tag{83}$$

It is interesting to note that the right side of the above inequality is equal to 45.0°, 63.4° and 78.6° for $\frac{b_{jk}}{g_{jk}}$ equal to 1, 2 and 5, respectively. Note that $\frac{b_{jk}}{g_{jk}}$ is normally greater than 5 (due to the specifications of the lines) and $\theta_{jk}^{\max}$ is normally less than 15° and very rarely as high as 30° due to stability and thermal limits (this angle constraint is forced either directly or through $p_{jk}^{\min}$ and $p_{jk}^{\max}$ in practice). Hence, Condition (83) is practical. Furthermore, each line of the power system can tolerate a certain amount of current in magnitude. One can verify that the magnitude of the current on the line (j,k), denoted by i_{jk}, satisfies the equation

$$|i_{jk}|^2 = |y_{jk}|\left(|v_j|^2 + |v_k|^2 - 2|v_j v_k|\cos(\theta_{jk})\right)$$

Therefore, an upper bound on $|i_{jk}|$ can be translated into a constraint on θ_{jk}, which can be reflected in $\theta_{jk}^{\max}$. By assuming that (83) is satisfied, there exists a monotonically decreasing, convex function $f_{jk}(\cdot)$ such that

$$p_{kj} = f_{jk}(p_{jk}), \quad \forall p_{jk} \in [p_{jk}^{\min}, p_{jk}^{\max}], \tag{84}$$

where $p_{jk}^{\min}$ and $p_{jk}^{\max}$ correspond to $\theta_{jk}^{\max}$ and $-\theta_{jk}^{\max}$, respectively.

Given two disparate edges (j,k) and (j',k'), the phase differences θ_{jk} and $\theta_{j'k'}$ may be varied independently in the distribution network. (84) implies that the problem of optimizing active flows reduces to GNF. In this case, Theorems 1 and 2 can be used to study the corresponding approximated OPF problem. As a result, the optimal injections for the approximated OPF can be found via the corresponding CGNF problem. This implies two facts about the conic relaxations studied in [19, 29–37] for solving the OPF problem:

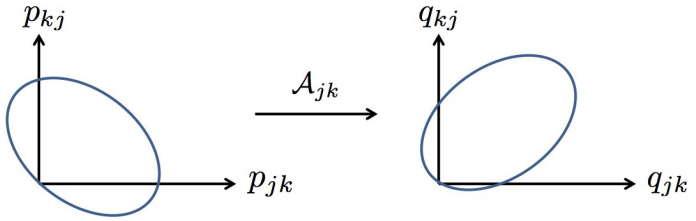

Fig. 11: Linear transformation of active flows to reactive flows

– The relaxations are exact without using the concept of load over-satisfaction (i.e., relaxing the flow constraints). This is a generalization of the results derived in the above papers (please refer to [37] for more details on this concept).
– Given the optimal injections, the optimal flows can be uniquely derived using the method delineated in the proof of Theorem 5.

In addition to active power, voltage magnitudes and reactive power are normally optimized in the OPF problem. In what follows, we generalize the above results to these cases.

3.6.1 Variable Reactive Power

In real-world power systems, different components of the network produce/consume reactive power. Since reactive power has a direct impact on the operation of the power system, this is often controlled in the OPF problem. To formulate the problem in this case, notice that each line has two reactive flows entering from its both endpoints. These equations can be described as

$$\begin{aligned} q_{jk} &= |v_j|^2 g_{jk} - |v_j||v_k| g_{jk} \sin(\theta_{jk}) - |v_j||v_k| b_{jk} \cos(\theta_{jk}), \\ q_{kj} &= |v_k|^2 g_{jk} + |v_j||v_k| g_{jk} \sin(\theta_{jk}) - |v_j||v_k| b_{jk} \cos(\theta_{jk}) \end{aligned} \tag{85}$$

Each bus at the network has a limited capacity to absorb/produce reactive power. Upon defining q_i as the reactive power injection at node i (which is equal to the summation of outgoing reactive flows from node i), this limited capacity can be captured by the pre-specified constraints $q_i^{\min} \leq q_i \leq q_i^{\max}$. Therefore, reactive flows can be written as linear functions of active flows based on the formula

$$\begin{bmatrix} q_{jk} \\ q_{kj} \end{bmatrix} = \underbrace{\frac{1}{2b_{jk}g_{jk}} \begin{bmatrix} b_{jk}^2 - g_{jk}^2 & b_{jk}^2 + g_{jk}^2 \\ b_{jk}^2 + g_{jk}^2 & b_{jk}^2 - g_{jk}^2 \end{bmatrix}}_{\mathcal{A}_{jk}} \begin{bmatrix} p_{jk} \\ p_{kj} \end{bmatrix} \tag{86}$$

Figure 11 visualizes this linear transformation. Assume that $\mathcal{G}$ is a tree (corresponding to a distribution network). Using (86), one can write the reactive power constraints in terms of the active flows. It can be observed that as long as the practical condition $\frac{b_{jk}}{g_{jk}} \geq 1$ is satisfied for every line (j,k), the upper

bound on the reactive power injection is a box-preserving convex constraint. This is due to the fact that each reactive power injection can be written as a linear and non-decreasing function of active flows (in light of (86)). This means that if the lower bounds on the reactive power injections are small enough (no matter what the upper bounds are), the OPF problem is reduced to the extended GNF problem with box-preserving coupling constraints. In this case, Theorem 6 can be invoked to conclude that the proposed convexification technique finds the optimal active-power injection vector. Similar to the previous case, once the optimal active-power injection vector is found, the optimal active and reactive flows can be uniquely extracted. It is worthwhile to mention that binding lower bounds on the reactive power injections may potentially destroy the exactness of the extended GNF problem since these constraints may not preserve the box property of the feasible region of the active-power injection vector.

3.6.2 Variable Voltage Magnitudes and Reactive Power

Consider the OPF problem with variable voltage magnitudes, namely $v_i^{\min} \leq |v_i| \leq v_i^{\max}$ for every node i in $\mathcal{G}$.

Definition 14 *Given an arbitrary line $(j,k) \in \mathcal{E}$, two numbers $u_j, u_k \in \mathbb{R}_+$, and an angle $\theta_{jk}^{\max} \in \mathbb{R}$, define $\mathcal{P}_{jk}(u_j, u_k, \theta_{jk}^{\max})$ as the set of all pairs (p_{jk}, p_{kj}) for which there exists an angle $-\theta_{jk}^{\max} \leq \theta_{jk} \leq \theta_{jk}^{\max}$ such that (85) holds after replacing $|v_j|$ and $|v_k|$ with u_j and u_k, respectively.*

We make the following assumptions:

- The set $\mathcal{P}_{jk}(u_j, u_k, \theta_{jk}^{\max})$ forms a monotonically decreasing curve in $\mathbb{R}^2$, for every line $(j,k) \in \mathcal{E}$ and the pair $(u_j, u_k) \in [v_j^{\min}, v_j^{\max}] \times [v_k^{\min}, v_k^{\max}]$.
- For every $[u_1, ..., u_{|\mathcal{N}|}] \in [v_1^{\min}, v_1^{\max}] \times ... \times [v_{|\mathcal{N}|}^{\min}, v_{|\mathcal{N}|}^{\max}]$, the OPF problem under the additional fixed-voltage-magnitude constraints $|v_i| = u_i, i = 1, ..., |\mathcal{N}|$ is feasible.

According to the first assumption, the upper bound on the angle difference between the two endpoints of each line must ensure that only the Pareto front of the ellipse describing the relationship between p_{jk} and p_{kj} is feasible. Notice that for every fixed set of voltages, (83) ensures that the first assumption is satisfied. Furthermore, the second assumption is practical since for every node i, the limits $v_i^{\min}$ and $v_i^{\max}$ are normally chosen to be less than $5-10\%$ away from the nominal voltage magnitudes.

Observe that the OPF problem for distribution networks (or acyclic graphs $\mathcal{G}$) can be reduced to the GNF problem after fixing the magnitude of every voltage at its optimal value. Since the CGNF is exact in this case, it can be shown that there is a second-order cone programming (SOCP) relaxation of the OPF problem with variable voltage magnitudes that is exact. This conic relaxation can be regarded as the union of the CGNF problems with different fixed voltage magnitudes. The details can be found in [56]. Furthermore, this conic relaxation is exact even in presence of reactive power constraints if the inequality $\frac{b_{jk}}{g_{jk}} \geq 1$ holds for every line of the network. The main reason is that

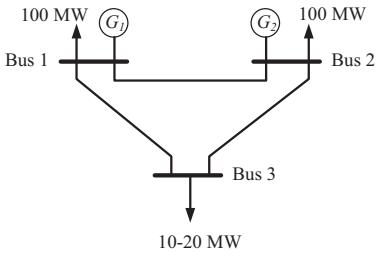

Fig. 12: The three-bus power network studied in Subsection 3.6.

the problem reduces to the one studied in the preceding subsection after fixing the voltage magnitudes at their optimal values.

3.6.3 OPF for General Networks

Given two different edges (j,k) and (j',k'), the phase differences θ_{jk} and $\theta_{j'k'}$ may not be varied independently if the graph $\mathcal{G}$ is cyclic (because the sum of the phase differences over a cycle must be zero). This is not an issue if the graph $\mathcal{G}$ is acyclic (corresponding to distribution networks) or if there is a sufficient number of phase-shifting transformers in the network. If none of these cases is true, then one could add virtual phase shifters to the power network at the cost of approximating the OPF problem. The following simple example is provided to further elaborate on the effect of this approximation.

Consider the three-bus network illustrated in Figure 12 with the node set $\mathcal{N} = \{1,2,3\}$, the edge set $\mathcal{E} = \{(1,2),(2,3),(3,1)\}$, and the line admittances (y):

$$y_{12} = 0.275 - 0.917\mathrm{i}, \quad y_{23} = 0.345 - 0.862\mathrm{i}, \quad y_{31} = 0.4 - 0.8\mathrm{i}$$

In this network, the loads at buses 1 and 2 are fixed at the value 100MW, whereas the load at bus 3 is flexible and can accept any amount of power in the range [10MW,20MW]. For simplicity, assume that the voltages are fixed at their nominal values and we only consider the active powers in the system. Furthermore, suppose that $\theta_{12}^{\max} = 40^\circ$, $\theta_{23}^{\max} = 50^\circ$ and $\theta_{31}^{\max} = 20^\circ$. Note that the angle constraint $|\theta_{jk}| \leq \theta_{jk}^{\max}$ can be regarded as the flow constraints $p_{jk}, p_{kj} \leq p_{jk}^{\max} = p_{kj}^{\max}$, where

$$p_{12}^{\max} = 71.29, \quad p_{23}^{\max} = 90.89, \quad p_{31}^{\max} = 37.21 \tag{87}$$

There are two generators in the system, whose active power outputs are denoted as P_{G_1} and P_{G_2}. Figure 13 represents the projection of the feasible set of OPF onto the space of the production vector (P_{G_1}, P_{G_2}) in two cases: (i) with no phase shifter, (ii) with a virtual phase shifter in the cycle. $\mathcal{P}$ is the feasible production region of (P_{G_1}, P_{G_2}). Define $\mathcal{P}_s$ as the projection of the feasible set of OPF problem onto the space for (P_{G_1}, P_{G_2}) after removing the angle constraint $\theta_{12} + \theta_{23} + \theta_{31} = 0$. The set $\mathcal{P}_s$ is depicted in Figure 13,

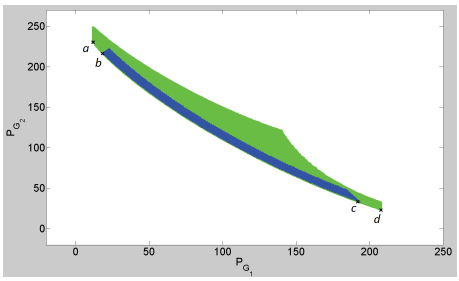

Fig. 13: Feasible set $\mathcal{P}$ (blue area) and feasible set $\mathcal{P}_s$ (blue and green areas).

which has two components: (i) the blue part $\mathcal{P}$, and (ii) the green part created by the elimination of the angle constraint. Four points have been marked on the Pareto front of $\mathcal{P}_s$ as a, b, c and d. Notice that the Pareto front of $\mathcal{P}_s$ has three segments:

- *Segment with the endpoints b and c:* This segment "almost" overlaps the Pareto front of $\mathcal{P}$. Indeed, there is a very little gap between this segment and the front of $\mathcal{P}$.
- *Segment with the endpoints a and b:* This segment extends the Pareto front of $\mathcal{P}$ from the top.
- *Segment with the endpoints c and d:* This segment extends the Pareto front of $\mathcal{P}$ from the bottom.

The gap between the Pareto front of $\mathcal{P}$ and a subset of the Pareto front of $\mathcal{P}_s$ with the endpoints b and c can be unveiled by performing some simulations. For instance, assume that $f_1(P_{G_1}) = P_{G_1}$ and $f_1(P_{G_2}) = 1.2P_{G_2}$. Two OPF problems will be solved next:

- *OPF without phase shifter:* The solution is $(P_{G_1}^{\text{opt}}, P_{G_2}^{\text{opt}}) = (144.27, 69.39)$ corresponding to the optimal cost \$227.53.
- *OPF with phase shifter:* The solution is $(P_{G_1}^{\text{opt}}, P_{G_2}^{\text{opt}}) = (145.56, 68.18)$ with $\theta_{12}^{\text{opt}} + \theta_{23}^{\text{opt}} + \theta_{31}^{\text{opt}} = 6.02^\circ$ corresponding to the optimal cost \$227.37.

Although the optimal value of the angle mismatch is not negligible, the optimal production $(P_{G_1}^{\text{opt}}, P_{G_2}^{\text{opt}})$ has very similar values in the above cases. In other words, the optimal injections obtained using the proposed convex problem are very close to the globally optimal solutions of OPF. Notice that the flows obtained from the convex problem could be completely wrong and one needs to pursue other techniques to find a set of optimal flows based on the obtained optimal injections.

The aforementioned case study offers a visual and intuitive explanation of the effect of virtual phase shifters on the optimal solution of the OPF problem and the Pareto front of the injection region. However, there is a large body of work suggesting that the inclusion of virtual phase shifters would have a small effect on the optimal solution of OPF in real-world systems [19, 49, 57–59]. Hence, the conclusion of this part is that the OPF problem with virtual phase

shifters can be efficiently converted to an SOCP problem (under mild assumptions), which leads to an approximate solution for OPF (to be later rectified in a local-search solver) or can be strengthened via convex constraints accounting for omitted phase cycle effects. For example, the paper [49] proposes a strengthened SOCP to solve the OPF problem, which exhibits a great performance in many systems. The above result implies that the success of the method developed in [49] is due in part to the fact that the SOCP relaxation correctly convefixies the OPF problem with virtual phase shifters, and therefore it eliminates some of the non-convexity of the original problem.

Several works in the literature indicate that the convex relaxation of the OPF and its related problems, such as voltage regulation [39] and the state estimation [42], are exact in most practical instances. This paper explains the reasoning behind the effectiveness of these methods by proposing a unified certificate on the exactness of these methods. In particular, it shows that these methods are successful under various conditions because the optimal solution belongs to the Pareto front of the feasible region and the proposed relaxations keep this Pareto front intact. One main application of this work is in the design of efficient algorithms for optimization over distribution networks, which is regarded as a key ingredient of future power systems, named Smart Grids. As a future work, the convexification of the GNF problem under a broader set of global coupling constraints (similar to the cycle effects in OPF) will be investigated. Another future direction is to study the GNF problem in the case where the injection and flow parameters are vectors of arbitrary dimensions, rather than scalars. This case naturally appears in multi-phased power systems, where the nodal injections (and line flows) are of dimension 1, 2 or 3. The machinery developed in this paper suggests that the GNF problem for such networks could be convefixied through the notion of CGNF if certain monotonicity and box-preserving properties are satisfied. A detailed analysis of these types of networks is left as future work.

4 Conclusions

Network flow plays a central role in operations research, computer science and engineering. Due to the complexity of this problem, the main focus has long been on lossless flow networks and more recently on networks with linear loss functions. This paper studies the generalized network flow (GNF) problem, which aims to optimize the flows over a lossy flow network. It is assumed that each node is associated with an injection and that the two flows at the endpoints of each line are related to each other via an arbitrary convex monotonic function. The GNF problem is hard to solve due to the presence of nonlinear equality flow constraints. It is shown that although GNF is highly nonconvex, globally optimal injections can be found by means of a convexified generalized network flow (CGNF) problem. It is also proven that CGNF obtains globally optimal flows for GNF, as long as the optimal injection vector is a Pareto point. In the case where CGNF returns a wrong (infeasible) flow vector for

GNF, the network can be decomposed into two subgraphs such that: (i) the flows found by CGNF for one of the subgraphs are all globally optimal, and (ii) the flows obtained by CGNF for the lines between the subgraphs are all correct and at their limits (i.e., the lines between the two subgraphs are congested). The set of all globally optimal flow vectors are characterized based on the optimal injection vector found using CGNF. This set may be infinite, non-convex, and disconnected, while it belongs to the boundary of a convex set. Finally, we generalize the GNF problem and its convexification to include coupling convex constraints on the flows or the injections. An immediate application of this work is in power systems, where the goal is to optimize the power flows at nodes and over lines of a power grid. Recent work on the optimal power flow problem has shown that this non-convex problem can be solved via a convex relaxation after two approximations: relaxing angle constraints (by adding virtual phase shifters) and relaxing power balance equations to inequality flow constraints. The results on GNF prove that the second approximation (on power balance equations) is redundant under a practical angle assumption.

References

1. A. V. Goldberg, E. Tardos, and R. E. Tarjan. Network flow algorithms. *Flows, Paths and VLSI (Springer, Berlin)*, pages 101–164, 1990.
2. W. S. Jewell. Optimal flow through networks with gains. *Operations Research*, 10:476–499, 1962.
3. L. R. Ford and D. R. Fulkerson. Flows in networks. *Princeton University Press*, 1962.
4. M. Klein. A primal method for minimal cost flows with applications to the assignment and transportation problems. *Management Science*, 14:205–220, 1967.
5. R. K. Ahuja, T. L. Magnanti, and J. B. Orlin. Network flows: theory, algorithms, and applications. *Prentice-Hall*, 1993.
6. D. Bertsimas and M. Sim. Robust discrete optimization and network flows. *Mathematical Programming*, 98:49–71, 2003.
7. D. Bertsimas and S. Stock-Paterson. The traffic flow management rerouting problem in air traffic control: A dynamic network flow approach. *Transportation Science*, 34:239–255, 2000.
8. M. S. Bazaraa, J. J. Jarvis, and H. D. Sherali. Linear programming and network flows. *John Wiley & Sons*, 1990.
9. J. Edmonds and R. M. Karp. Theoretical improvements in algorithmic efficiency for network flow problems. *Journal of the ACM*, 19:248–264, 1972.
10. K. E. Nygard, P. R. Chandler, and M. Pachter. Dynamic network flow optimization models for air vehicle resource allocation. *American Control Conference*, 2001.
11. D. Goldfarb and J. Hao. Polynomial-time primal simplex algorithms for the minimum cost network flow problem. *Algorithmica*, 8:145–160, 1992.
12. D. Bienstock, S. Chopra, O. Gunluk, and C. Y. Tsai. Minimum cost capacity installation for multicommodity network flows. *Mathematical Programming*, 81:177–199, 1998.
13. H. Brannlund, J. A. Bubenko, D. Sjelvgren, and N. Andersson. Optimal short term operation planning of a large hydrothermal power system based on a nonlinear network flow concept. *IEEE Transactions on Power Systems*, 1:75–81, 1986.
14. J. L. Goffin, J. Gondzio, R. Sarkissian, and J. P. Vial. Solving nonlinear multicommodity flow problems by the analytic center cutting plane method. *Mathematical Programming*, 76:131–154, 1996.
15. S. Boyd and L. Vandenberghe. *Convex Optimization.* Cambridge, 2004.

16. M. Kraning, E. Chu, J. Lavaei, and S. Boyd. Dynamic network energy management via proximal message passing. *Foundations and Trends in Optimization*, 1(2):1–54, 2013.
17. A. Araposthatis, S. Sastry, and P. Varaiya. Analysis of power-flow equation. *International Journal of Electrical Power & Energy Systems*, 3:115–126, 1981.
18. I. A. Hiskens and R. J. Davy. Exploring the power flow solution space boundary. *IEEE Transactions on Power Systems*, 16(3):389–395, 2001.
19. S. Sojoudi and J. Lavaei. Physics of power networks makes hard optimization problems easy to solve. *IEEE Power & Energy Society General Meeting*, 2012.
20. J. Carpentier. Contribution to the economic dispatch problem. *Bulletin Society Francaise Electriciens*, 1962.
21. H. W. Dommel and W. F. Tinney. Optimal power flow solutions. *IEEE Transactions on Power Apparatus and Systems*, 1968.
22. J. A. Momoh, M. E. El-Hawary, and R. Adapa. A review of selected optimal power flow literature to 1993. Part I: Nonlinear and quadratic programming approaches. *IEEE Transactions on Power Systems*, 1999.
23. J. A. Momoh, M. E. El-Hawary, and R. Adapa. A review of selected optimal power flow literature to 1993. Part II: Newton, linear programming and interior point methods. *IEEE Transactions on Power Systems*, 1999.
24. T. J. Overbye, Xu Cheng, and Yan Sun. A comparison of the AC and DC power flow models for LMP calculations. In *Proceedings of the 37th Hawaii International Conference on System Sciences*, 2004.
25. R. Baldick. *Applied Optimization: Formulation and Algorithms for Engineering Systems*. Cambridge, 2006.
26. K. S. Pandya and S. K. Joshi. A survey of optimal power flow methods. *Journal of Theoretical and Applied Information Technology*, 2008.
27. R. A. Jabr. Optimal power flow using an extended conic quadratic formulation. *IEEE Transactions on Power Systems*, 23(3):1000–1008, 2008.
28. Y. V. Makarov, Z. Y. Dong, and D. J. Hill. On convexity of power flow feasibility boundary. *IEEE Transactions on Power Systems*, 2008.
29. J. Lavaei and S. H. Low. Zero duality gap in optimal power flow problem. *IEEE Transactions on Power Systems*, 27(1):92–107, 2012.
30. R. Madani, S. Sojoudi, and J. Lavaei. Convex relaxation for optimal power flow problem: Mesh networks. *IEEE Transactions on Power Systems*, 30(1):199–211, 2015.
31. R. Madani, M. Ashraphijuo, and J. Lavaei. Promises of conic relaxation for contingency-constrained optimal power flow problem. *IEEE Transactions on Power Systems*, 31(2):1297–1307, 2016.
32. S. Sojoudi and J. Lavaei. Exactness of semidefinite relaxations for nonlinear optimization problems with underlying graph structure. *SIAM Journal on Optimization*, 24(4):1746–1778, 2014.
33. B. Lesieutre, D. Molzahn, A. Borden, and C. L. DeMarco. Examining the limits of the application of semidefinite programming to power flow problems. *49th Annual Allerton Conference*, 2011.
34. S. Bose, D. F. Gayme, S. Low, and M. K. Chandy. Optimal power flow over tree networks. *Proceedings of the Forty-Ninth Annual Allerton Conference*, 2011.
35. B. Zhang and D. Tse. Geometry of injection regions of power networks. *IEEE Transactions on Power Systems*, 28(2):788–797, 2013.
36. J. Lavaei, B. Zhang, and D. Tse. Geometry of power flows in tree networks. *IEEE Power & Energy Society General Meeting*, 2012.
37. J. Lavaei, D. Tse, and B. Zhang. Geometry of power flows and optimization in distribution networks. *IEEE Transactions on Power Systems*, 29(2):572–583, 2014.
38. J. Lavaei and S. H. Low. Convexification of optimal power flow problem. *48th Annual Allerton Conference*, 2010.
39. A. Y. S. Lam, B. Zhang, A. Dominguez-Garcia, and D. Tse. An optimal and distributed method for voltage regulation in power distribution systems. *IEEE Transactions on Power Systems*, 30(4):1714–1726, 2015.
40. D. Gayme and U. Topcu. Optimal power flow with large-scale storage integration. *IEEE Transactions on Power Systems*, 28(2):709–717, 2013.
41. Y. Weng, Q. Li, R. Negi, and M. Ilic. Semidefinite programming for power system state estimation. *IEEE Power & Energy Society General Meeting*, 2012.

42. R. Madani, J. Lavaei, and R. Baldick. Convexification of power flow equations for power systems in presence of noisy measurements. *http://www.ieor.berkeley.edu/~lavaei/SE_J_2016.pdf*, 2016.
43. V. Kekatos, G. B. Giannakis, and B. Wollenberg. Optimal placement of phasor measurement units via convex relaxation. *IEEE Transactions on power systems*, 27(3):1521–1530, 2012.
44. D. K. Molzahn, B. C. Lesieutre, and C. L. DeMarco. A sufficient condition for power flow insolvability with applications to voltage stability margins. *IEEE Transactions on Power Systems*, 28(3):2592–2601, 2013.
45. S. Sojoudi and S. H. Low. Optimal charging of plug-in hybrid electric vehicles in smart grids. *IEEE Power & Energy Society General Meeting*, 2011.
46. J. Lavaei. Zero duality gap for classical OPF problem convexifies fundamental nonlinear power problems. *American Control Conference*, 2011.
47. J. Lavaei and S. Sojoudi. Competitive equilibria in electricity markets with nonlinearities. *American Control Conference*, 2012.
48. H. Hijazi, C. Coffrin, and P. V. Hentenryck. Convex quadratic relaxations for mixed-integer nonlinear programs in power systems. *Mathematical Programming Computation*, pages 1–47, 2013.
49. B. Kocuk, S. S. Dey, and X. A. Sun. Strong SOCP relaxations for the optimal power flow problem. *Operations Research*, 64(6):1177–1196, 2016.
50. S. Fattahi, M. Ashraphijuo, J. Lavaei, and A. Atamturk. Conic relaxations of the unit commitment problem. Under review for *Energy* (conference version appeared in CDC 2016), available online at `http://www.ieor.berkeley.edu/~lavaei/UC_Conic_2016.pdf`, 2016.
51. R. P. O'Neill, R. Baldick, U. Helman, M. H. Rothkopf, and W. Stewart. Dispatchable transmission in rto markets. *IEEE Transactions on Power Systems*, 20(1):171–179, 2005.
52. C. Josz, J. Maeght, P. Panciatici, and J. C. Gilbert. Application of the moment-SOS approach to global optimization of the OPF problem. *IEEE Transactions on Power Systems*, 30(1):463–470, 2015.
53. D. Molzahn, C. Josz, I. Hiskens, and P Panciatici. Solution of optimal power flow problems using moment relaxations augmented with objective function penalization. *IEEE Conference on Decision and Control (CDC)*, pages 31–38, 2015.
54. J. B. Lasserre. Global optimization with polynomials and the problem of moments. *SIAM Journal on Optimization*, 11(3):796–817, 2001.
55. R. Madani, S. Sojoudi, G. Fazelnia, and J. Lavaei. Finding low-rank solutions of sparse linear matrix inequalities using convex optimization. to appear in *SIAM Journal on Optimization,* available online at `http://www.ieor.berkeley.edu/~lavaei/LMI_Low_Rank.pdf`, 2017.
56. S. Sojoudi and J. Lavaei. Convexification of optimal power flow problem by means of phase shifters. In *IEEE International Conference on Smart Grid Communications*, pages 756–761, 2013.
57. M. Farivar and S. H. Low. Branch flow model: Relaxations and convexification—Part II. *IEEE Transactions on Power Systems*, 28(3):2565–2572, 2013.
58. S. H. Low. Convex relaxation of optimal power flow—Part I: Formulations and equivalence. *IEEE Transactions on Control of Network Systems*, 1(1):15–27, 2014.
59. S. H. Low. Convex relaxation of optimal power flow—Part II: Exactness. *IEEE Transactions on Control of Network Systems*, 1(2):177–189, 2014.